TABLE 1. Strains and plasmids used in this study

Strain or plasmid	Relevant genotype and/or description	Source; reference(s)[a]
Strains		
AB1157	Wild type	K. Yamamoto; 79
YG2238	AB1157 ΔKlenow::*cat*	T. Nohmi; 76
YG6341	AB1157 Δ*polB*::*kan*	This study
YG6158	AB1157 Δ*dinB*::*kan*	This study
YG6162	AB1157 Δ*dinB*	This study
YG6168	AB1157 Δ(*umuDC*)*596*::*ermGT*	This study
YG6171	AB1157 Δ*dinB* Δ(*umuDC*)*596*::*ermGT*	This study
YG6342	YG6168 Δ*dinB* Δ*polB*::*kan*	This study
YG6344	YG6342 ΔKlenow::*cat*	This study
NKJ1514	AB1157 *recQ*::Tn*3*	This study
NKJ1515	AB1157 *recJ*::Tn*10*	This study
KY1056	AB1157 *recA56 srlC300*::Tn*10*	K. Yamamoto; 79
ME8083	AB1157 *recB21*	NBRP; 30
IP10	AB1157 *recF*::*tet*	M. Bichara; 6
C266	AB1157 *recG258*::*kan*	M. G. Marinus; 37
HRS2300	AB1157 *ruvA100*::*cat*	T. Hishida; 27
HRS1200	AB1157 Δ*ruvC200*::*kan*	T. Hishida; 34
KY1836	AB1157 *uvrA6*	K. Yamamoto; 1
AB1885	AB1157 *uvrB5*	K. Yamamoto; 29
NKJ1500	AB1157 *uvrC279*::Tn*10*	This study
RPC501	AB1157 Δ(*xthA-pncA*) *nfo-1*::*kan*	S. Yonei; 13
BH20	AB1157 *fpg-1*::*kan*	K. Yamamoto; 8
NKJ1004	AB1157 *nth*::*cat* Δ*nei*::*kan*	K. Yamamoto; 60
KL16	Wild type (BW35)	S. S. Wallace; 7
KL16 *nei nth fpg*	KL16 *nei*::*cat nth*::*kan fpg*::*amp*	S. S. Wallace; 7
AQ10459	Wild type	NBRP; 36
AQ10479	AQ10459 *priA2*::*kan*	NBRP; 36
DM4000	Wild type	S. J. Sandler; 63
JC19266	DM4000 Δ(*priB*)*302*	S. J. Sandler; 63
JC19165	DM4000 *priC303*::*kan*	S. J. Sandler; 63
JJC213	JJC40 *rep*::*kan*	S. J. Sandler; 63
MG1655	Wild type	R. G. Lloyd; 72
N4879	MG1655 Δ*mfd*::*kan*	R. G. Lloyd; 72
N5301	MG1655 *greA*::*cat*	R. G. Lloyd; 72
N5753	MG1655 Δ*dksA*::*apra*	R. G. Lloyd; 72
KMBL1001	F^- derivative of W1485	N. Goosen; 48
CS5541	KMBL1001 Δ*cho* (FRT)	N. Goosen; 48
CS5430	KMBL1001 Δ*uvrC*::*cat*	N. Goosen; 48
CS5550	KMBL1001 Δ*cho* (FRT) Δ*uvrC*::*cat*	N. Goosen; 48
CS5431	KMBL1001 Δ*uvrD*::*tet*	N. Goosen; 48
RFM443	Wild type	M. Drolet; 17
RFM445	RFM443 *gyrB221* (Cou^r) *gyrB203*(Ts)	M. Drolet; 17
RFM475	RFM443 *gyrB221* (Cou^r) *gyrB203*(Ts) Δ(*topA cysB*)204	M. Drolet; 17
BIK814	*recJ*::Tn*10*	K. Yamamoto; 71
KD2250	*recQ*::Tn*3*	K. Yamamoto; 53
HRS7052[b]	ΔKlenow::*cat*	H. Iwasaki; 35, 76
HRS6700	Δ*polB*::*kan*	H. Iwasaki; 67
DE2302	Δ(*umuDC*)*595*::*cat fadR615*::Tn*10 purB58*	R. Woodgate; 78
EC8	Δ(*umuDC*)*596*::*ermGT fadR purB*$^+$	R. Woodgate; 19
CAG12156	*uvrC279*::Tn*10*	K. Yamamoto; 68
Plasmids		
pKD13	Encodes Kan^r cassette flanked by FRT sequences, temperature sensitive; Kan^r Amp^r	CGSC
pKD46	Encodes the lambda Red system under the control of arabinose-promoter, temperature sensitive; Amp^r	CGSC
pCP20	Encodes a recombinase, FLP, temperature sensitive; Amp^r Cam^r	CGSC
pNTR-SD-Dcm	pNTR-SD containing the IPTG-inducible *dcm* gene	NBRP; 61

[a] NBRP, National BioResource Project; CGSC, Coli Genetic Stock Center.
[b] HRS7052 was derived from the strain described in reference 35.

sensitivities of the *priB* and *priC* mutants suggest that the PriA-PriB pathway contributes more to RR than the PriA-PriC pathway does, but the two pathways can compensate for each other to a significant degree when one is compromised. In addition to the PriA-dependent RR pathways, there is an alternative Rep-PriC restart pathway to load DnaB onto the forked DNA structures (63). However, the *rep* mutant was sensitive to neither FA nor azaC (Fig. 1C and F), indicating that the Rep-PriC pathway is dispensable in RR following the HR of DPCs.

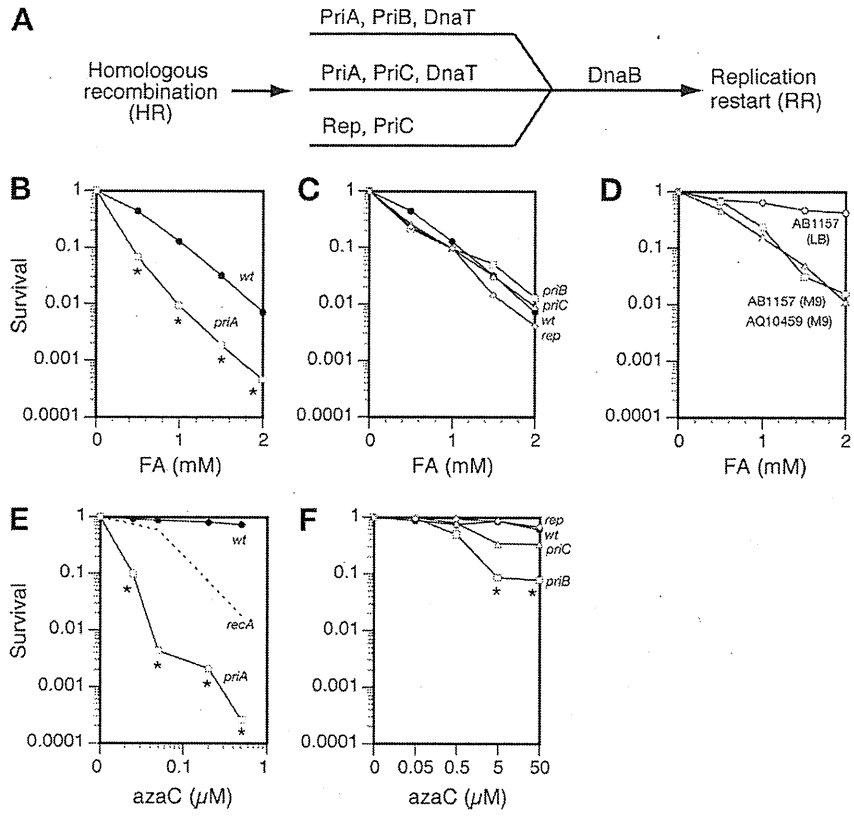

FIG. 1. Survival of RR mutants after treatment with FA and azaC. (A) Three RR pathways in *E. coli*. Two pathways are PriA dependent and the other is PriA independent and requires the Rep helicase. (B) FA treatment. Shown are AQ10459 (wt) (filled circles) and *priA* (squares). (C) FA treatment. Shown are data for DM4000 (wt) (filled circles) and the *priB* (squares), *priC* (triangles), and *rep* (diamonds) mutants. (D) Comparison of FA sensitivities of AB1157 and AQ10459 in LB and M9 media. Shown are data for AB1157 in LB (circles) and M9 (squares) media and AQ10459 in M9 (triangles) medium. Data for AQ10459 were taken from that shown in panel B, and those for AB1157 are based on one experiment. (E and F) azaC treatment. Symbols represent the same strains as shown in panels B and C, respectively. For a comparison, the survival curve of *recA* (data taken from that shown in Fig. 2B) is also shown by the broken line in panel E. In panels B, C, E, and F, cells were treated with FA and azaC in M9 medium. Data points showing statistically significant differences ($P < 0.05$) between the wt and the mutant are indicated with asterisks. Note that azaC concentrations are displayed on a logarithmic scale.

We used M9 as a common medium for the FA treatment of RR mutants (Fig. 1B and C), since one of the RR mutants used (*priA*) is sensitive to rich media (36). Conversely, rich LB medium was used for the FA treatment of the other sets of mutants (Fig. 2 to 5). The use of M9 medium significantly increased the FA sensitivity of cells. For instance, AB1157 (wt) was more sensitive in M9 medium than in LB medium, with the sensitivity in M9 being comparable to that of AQ10459 (wt) in M9 medium (Fig. 1D). Thus, FA concentrations used in the survival assays of RR mutants (0 to 2 mM) (Fig. 1B and C) were lower than those used for other sets of mutants (0 to 7 mM or 0 to 16 mM) (Fig. 2 to 5). In view of the high reactivity of FA to amino and sulfhydryl compounds, it is likely that the constituents of rich LB medium scavenged FA more effectively than those of M9 medium. The azaC sensitivity of RR mutants was also assayed in M9 medium. The azaC concentrations used for the *priB*, *priC*, and *rep* mutants were the same as those used for other sets of mutants (Fig. 2 to 5). However, azaC concentrations used for the *priA* mutant were much lower than those for other sets of mutants due to an extreme sensitivity of the mutant. The *priA* mutant was hypersensitive to both FA and azaC, but the sensitivity to azaC was by far greater than that to FA (Fig. 1B and E). Also, the *priA* mutant grew very slowly (see Table S1 in the supplemental material) and was more sensitive to azaC than the *recA* mutant (Fig. 1E). Taken together, it is likely that the extreme azaC sensitivity of the *priA* mutant exhibiting complex phenotypes is attributable to defects not only in RR but also in yet-unknown factors.

Overproduction of Dcm increases azaC sensitivity of cells. We have previously proposed that DPCs containing large cross-linked proteins (>12 to 14 kDa) are not repaired by NER and exclusively processed by RecBCD-dependent HR that involves the genes *recA*, *recBCD*, *recG*, and *ruvABC*. We confirmed that these mutants were sensitive to FA, whereas the *recF* mutant was not (see Fig. S2A in the supplemental material). azaC incorporated into the chromosome likely traps the Dcm protein (53 kDa), giving rise to large DPCs (Dcm-DPCs) that are exclusively processed by RecBCD-dependent HR. Consistent with this mechanism, it was reported that overproduction of the Dcm protein from the *dcm*-carrying plasmid increased the azaC sensitivity of wt cells by 930-fold and increased that of the *recA* mutant by fivefold (5). However,

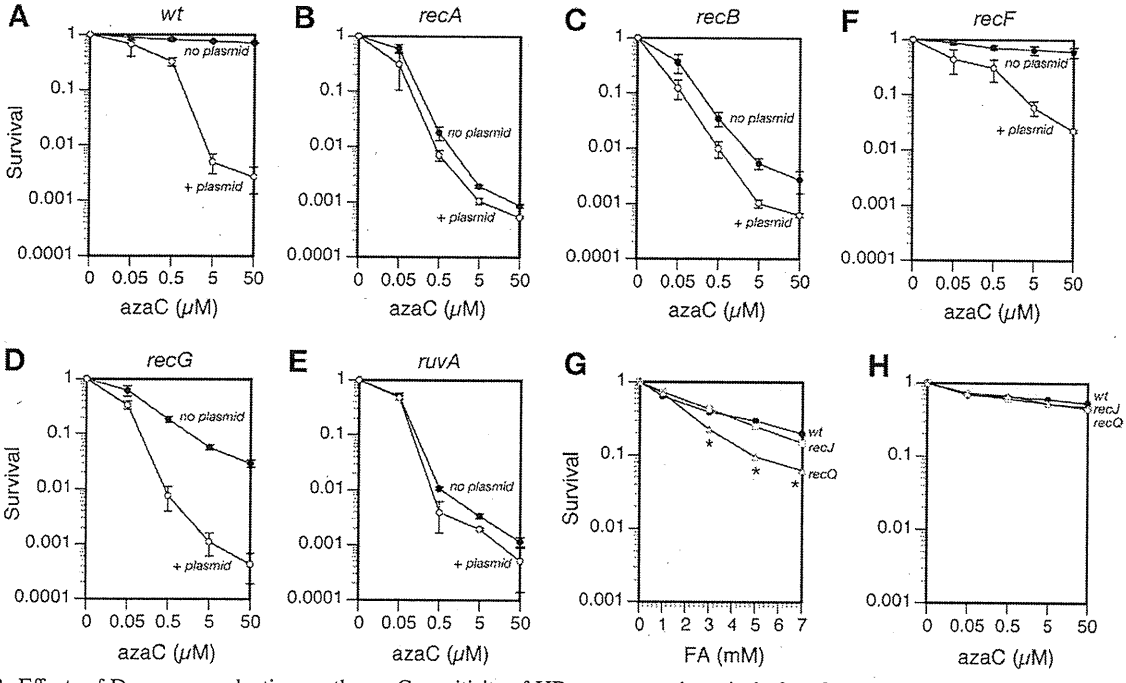

FIG. 2. Effects of Dcm overproduction on the azaC sensitivity of HR mutants and survival of *recQ* and *recJ* mutants after treatment with FA and azaC. (A to F) Effects of Dcm overproduction on the azaC sensitivity of HR mutants. AB1157 (wt) and HR mutants (*recA*, *recB*, *recF*, *recG*, and *ruvA*) harboring pNTR-SD-Dcm (open circles) or no plasmid (filled circles) were treated with 1 mM IPTG for 10 min, followed by azaC in minimal A medium. HR mutants used were KY1056 (*recA*), ME8083 (*recB*), IP10 (*recF*), C266 (*recG*), and HRS2300 (*ruvA*). Standard deviations are indicated with error bars. (G and H) FA and azaC treatment of *recQ* and *recJ*. Shown are data for AB1157 (wt) (filled circles) and the *recJ* (squares), and *recQ* (triangles) mutants. Cells were treated with FA and azaC in LB and minimal A media, respectively. Data points showing statistically significant differences ($P < 0.05$) between the wt and the mutant are indicated with asterisks. Note that azaC concentrations are displayed on a logarithmic scale.

interestingly, the same report showed that the *dcm* mutant was not particularly resistant to azaC compared to the corresponding wt cell that expressed a physiological level of Dcm (5). Our tentative interpretation of the apparently inconsistent results regarding the effects of overproduction and mutational inactivation of Dcm is that the HR capacity of the repair-proficient wt cells is sufficient enough to deal with Dcm-DPCs produced from endogenous Dcm. Using the fluorescein isothiocyanate-labeling method (51), we attempted to detect Dcm-DPCs in DNA isolated from azaC-treated cells without success (data not shown), suggesting very low levels of the endogenous Dcm protein and concomitant Dcm-DPCs in cells. To confirm the role of HR in the processing of Dcm-DPCs more clearly, we used cells harboring pNTR-SD-Dcm, which overproduces the Dcm protein upon treatment with IPTG. A similar approach has shown that overproduction of EcoRII Dcm results in the

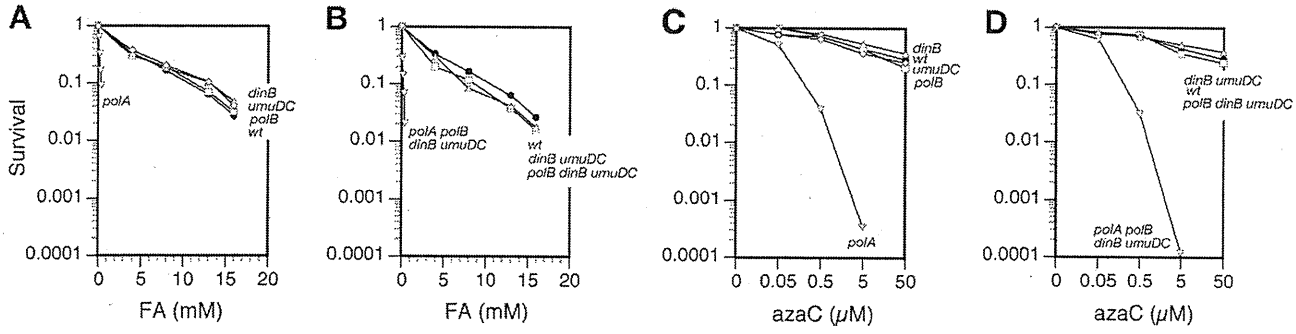

FIG. 3. Survival of TLS mutants after treatment with FA and azaC. (A) FA treatment of single mutants. Shown are data for AB1157 (wt) (filled circles) and the *polB* (squares), *dinB* (triangles), *umuDC* (diamonds), and *polA* (inverted triangles) mutants. (B) FA treatment of mutants defective in multiple polymerases. Shown are data for AB1157 (wt) (filled circles) and the *dinB umuDC* (squares), *polB dinB umuDC* (triangles), and *polA polB dinB umuDC* (inverted triangles) mutants. (C and D) azaC treatment of single mutants and those defective in multiple polymerases, respectively. Symbols represent the same strains as shown in panels A and B, respectively. Cells were treated with FA and azaC in LB and minimal A media, respectively. Except for mutants containing the *polA* mutation, there were no statistically significant differences in cell survival between the wt and the TLS mutants. Note that azaC concentrations are displayed on a logarithmic scale.

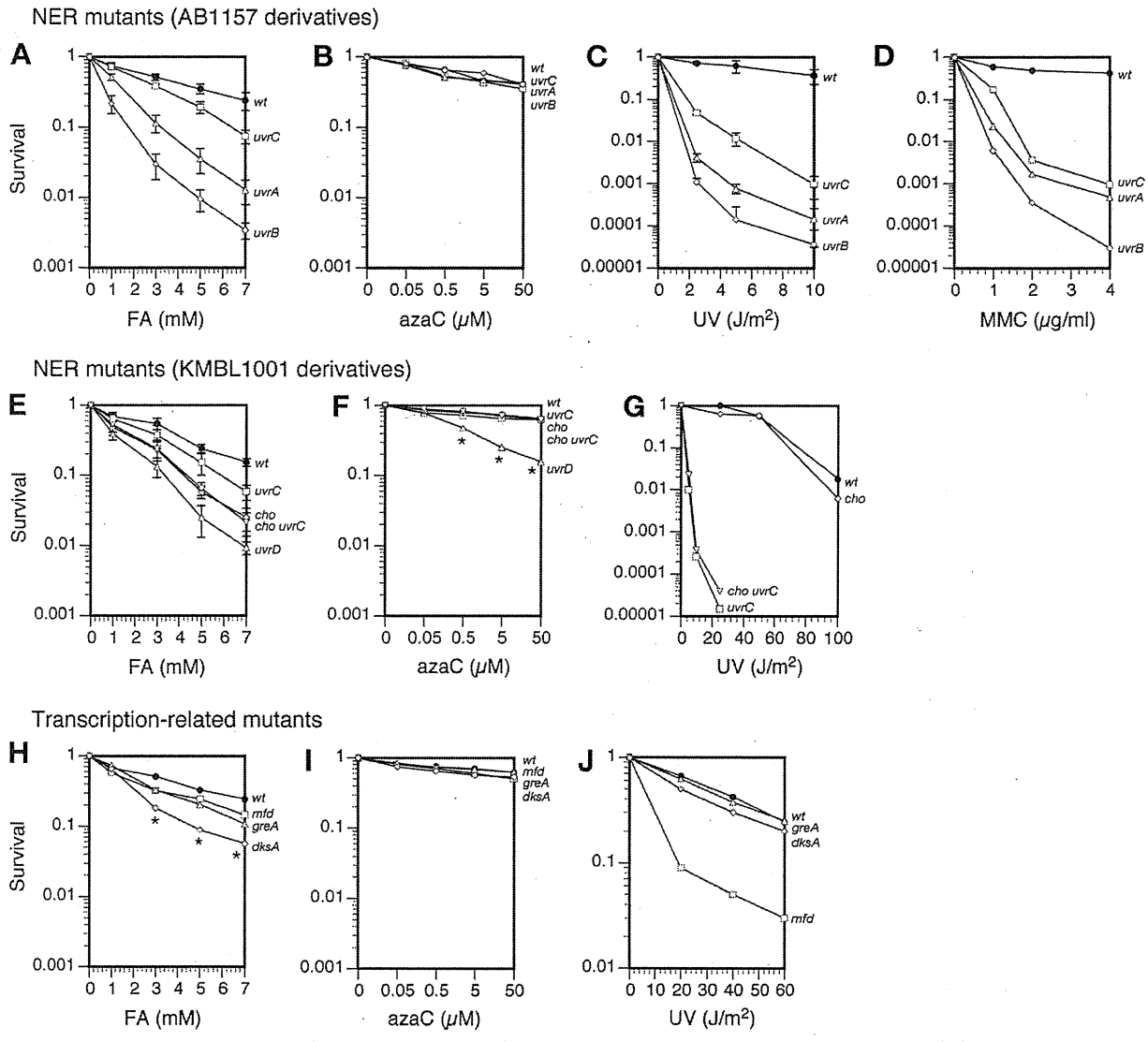

FIG. 4. Survival of NER and transcription-related mutants after treatment with FA, azaC, UV light, or MMC. Cells were treated with indicated agents. (A to D) NER mutants derived from AB1157. Shown are the wt (filled circles), *uvrA* (triangles), *uvrB* (diamonds), and *uvrC* (squares). (E to G) NER mutants derived from KMBL1001. Shown are data for the wt (filled circles) and the *uvrC* (squares), *uvrD* (triangles), *cho* (diamonds), and *cho uvrC* (inverted triangles) mutants. (H to J) Transcription-related mutants. Shown are data for MG1655 (wt) (filled circles) and the *mfd* (squares), *greA* (triangles), and *dksA* (diamonds) mutants. Standard deviations are indicated with error bars to show the statistically significant sensitivity differences between mutants shown in panels A, C, and E. Also, data points showing statistically significant differences ($P < 0.05$) between the wt and the mutant are indicated with asterisks in panels F and H. Data in panels D, G, and J are based on one or two experiments.

replication arrest of plasmid pBR322 at the canonical methylation site in *E. coli* cells grown in the presence of azaC (38). Overproduction of Dcm from a plasmid dramatically increased the azaC sensitivity of cells that were insensitive (wt and *recF*) or moderately sensitive (*recG*) to azaC without a plasmid (Fig. 2A, F, and D). Similarly, overproduction of Dcm slightly increased the azaC sensitivity of *recA*, *recB*, and *ruvA* mutants that were hypersensitive to azaC without a plasmid (Fig. 2B, C, and E). We infer that the HR of *recA*, *recB*, and *ruvA* mutants was severely impaired so that Dcm-DPCs produced from endogenous Dcm were sufficient to kill the mutants. Thus, overproduction of Dcm-DPCs in the mutants did not result in a dramatic increase in cell killing.

RecQ, but not RecJ, is slightly sensitive to FA. The RecQ helicase and RecJ exonuclease are the components of the RecFOR recombination machinery (39). The *recJ* mutant was sensitive to neither FA nor azaC (Fig. 2G and H). The *recQ* mutant displayed no sensitivity to azaC (Fig. 2H) but was slightly sensitive to FA (Fig. 2G). Although the FA sensitivity of the *recQ* mutant was significant, the phenotype to FA was by far milder than that of the *recB* mutant (see Fig. S2A in the supplemental material and reference 51). Accordingly, this is consistent with our previous observation that DPCs are processed exclusively by RecBCD-dependent HR and not RecFOR-dependent HR (51). In addition to its role in the RecFOR pathway, RecQ is suggested to be involved in SOS DNA

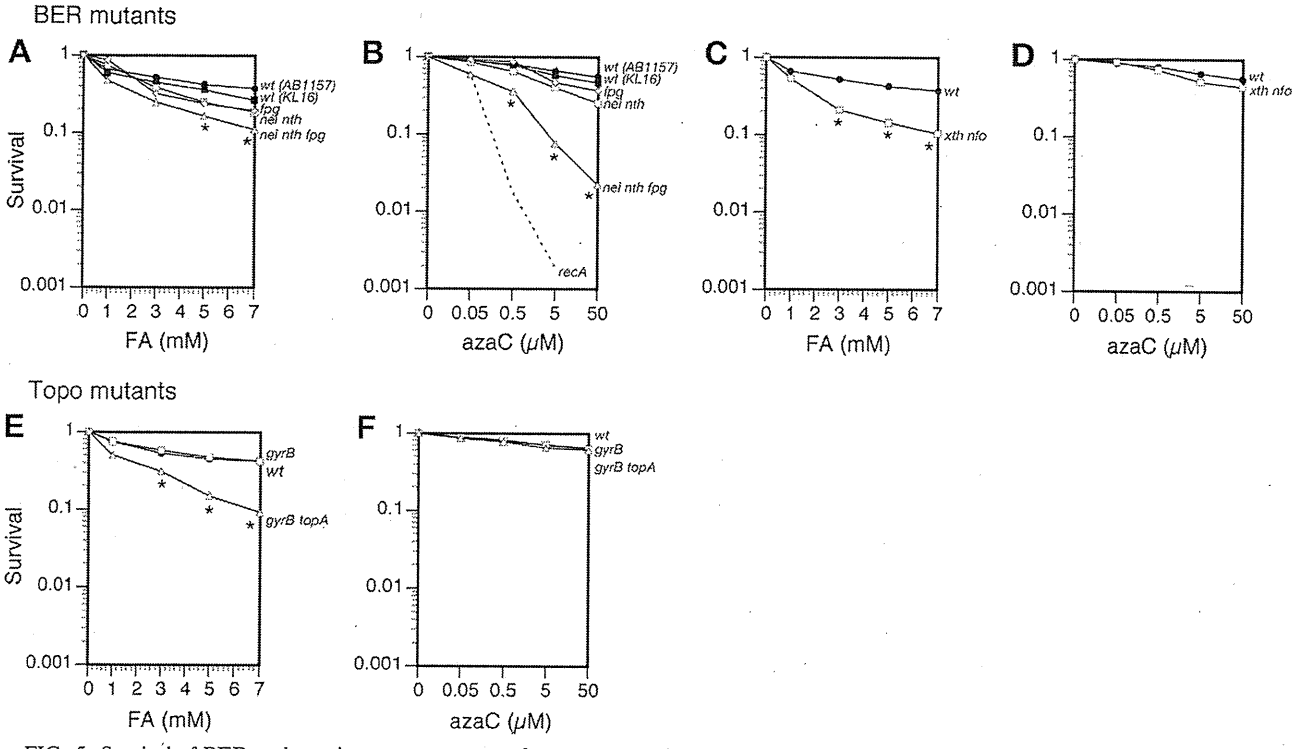

FIG. 5. Survival of BER and topoisomerase mutants after treatment with FA and azaC. Cells were treated with indicated agents. (A and B) DNA glycosylase mutants. AB1157 derivatives are as follows: wt (filled circles), *fpg* (diamonds), and *nei nth* (squares). KL16 derivatives are as follows: wt (filled squares) and *nei nth fpg* (triangles). For a comparison, the survival curve of *recA* (data taken from that shown in Fig. 2B) is also shown by the broken line in panel B. (C and D) AP endonuclease mutants. Shown are data for AB1157 (wt) (filled circles) and the *xth nfo* (squares) mutant. (E and F) Topoisomerase mutants. Shown are data for RFM443 (wt) (filled circles) and the *gyrB* (squares), and *gyrB topA* (triangles) mutants. Data points showing statistically significant differences ($P < 0.05$) between the wt and the mutant are indicated with asterisks.

damage signaling in response to replication fork stalling (26). However, it is not clear whether the weak FA sensitivity of the *recQ* mutant is related to SOS damage signaling.

TLS provides no alternative damage tolerance pathway to DPCs. The presence of a lesion in template DNA often causes the replicative DNA polymerase to stall at the lesion. *E. coli* cells possess TLS DNA polymerases (Pol), including Pol II (*polB*), Pol IV (*dinB*), and Pol V (*umuDC*), that can transiently take over from the replicative polymerase to continue synthesis across the lesion, allowing replication to resume (55). With UV-induced lesions, there are conflicting reports on the role of Pol II in RR. Pol II was originally implicated in RR (57), but this possibility was ruled out by a subsequent study (11). Interestingly, Pol V becomes essential for RR in the absence of RecJ and RecQ, although the role of Pol V in RR is modest in wt cells (12). To ask whether TLS polymerases play any significant role in the resumption of replication, and hence contribute to damage tolerance to DPCs, the FA and azaC sensitivities of TLS polymerase mutants (*polB*, *dinB*, and *umuDC*) were assayed. The single mutants exhibited no sensitivity to FA or azaC (Fig. 3A and C). Moreover, the double (*dinB umuDC*) and triple (*polB dinB umuDC*) mutants were not sensitive to FA and azaC at all (Fig. 3B and D). These results clearly indicate that neither direct TLS nor indirect TLS involving template switching (23, 25) provides an alternative damage tolerance pathway to DPCs with respect to cell survival. In contrast, the *polA* mutants deficient in Pol I (YG2238 and YG6344) were hypersensitive to both FA and azaC (Fig. 3A to D). These results demonstrate the essential role of Pol I as a repair polymerase both in NER and HR.

NER mutants exhibit various degrees of FA and azaC sensitivity. We have previously shown that the *uvrA* mutant is sensitive to FA but not azaC, demonstrating that NER partly contributes to the repair of FA-induced DPCs. Here we assessed the roles of a series of NER genes, including *uvrA*, *uvrB*, *uvrC*, *uvrD*, *cho*, and *mfd* (73), and those of repair-related transcription factors, including *dksA* and *greA* (72), in the processing of DPCs. We confirmed the moderate UV sensitivity of the *mfd* mutant (Fig. 4J) (66) and the lack thereof of the *cho* mutant (Fig. 4G) (48). The mutants were treated with FA and azaC, and their sensitivities were determined.

For analysis of NER genes, we used two sets of mutants derived from AB1157 and KMBL1001. With AB1157 derivatives, the mutants involved in damage recognition (*uvrA* and *uvrB*) and the dual incision of DNA (*uvrC*) were sensitive to FA, but their sensitivities differed significantly from each other (*uvrB* > *uvrA* > *uvrC*) (Fig. 4A). The mutants were also sensitive to UV and MMC (Fig. 4C and D), and shared a common order of sensitivity to FA, UV, and MMC (*uvrB* > *uvrA* > *uvrC*). However, the *uvrC* mutant exhibited a uniquely weak sensitivity to FA but not UV and MMC. The uniquely weak FA sensitivity characteristic of the *uvrC* mutant was confirmed

using another set of strains derived from KMBL1001 (Fig. 4E). Conversely, the *cho* mutant exhibited a moderate sensitivity to FA (Fig. 4E), suggesting its in vivo role as an alternative nuclease in the NER of DPCs (see Discussion). To our knowledge, this is the first report of the phenotype of the *cho* single mutant to DNA-damaging agents. The *cho uvrC* double mutant exhibited an FA sensitivity comparable to that of the *cho* single mutant (Fig. 4E). Consistent with its role in NER, the *uvrD* mutant was sensitive to FA (Fig. 4E), indicating that the UvrD helicase can unwind the duplex containing DPC and dissociate the DPC-containing fragment from its complementary strand. Unlike *uvrA*, *uvrB*, *uvrC*, and *cho* mutants that were not sensitive to azaC (Fig. 4B and F), the *uvrD* mutant displayed a slight but statistically significant sensitivity to azaC as well (Fig. 4F), suggesting a role of UvrD outside NER (see Discussion). Mfd is a transcription-coupled repair (TCR) factor that translocates RNA polymerase stalled at the lesion, recruiting UvrA to the site (66, 73). However, the *mfd* mutant exhibited no sensitivity to FA and azaC (Fig. 4H and I), indicating that unlike the pyrimidine photodimers that are repaired through both global genome repair and TCR pathways, DPCs are eliminated from the genome by global genome repair-NER exclusively.

In *E. coli*, it has been shown that the backed-up arrays of stalled transcription complexes which are impediments to replication are kept under surveillance of the stringent response regulators ppGpp and DksA or the GreA and Mfd proteins, which revive or dislodge stalled transcription complexes (72). Thus, it would be interesting to determine whether transcription complexes stalled by DPCs are under such a surveillance system. To clarify this, the sensitivities of the *dksA* and *greA* mutants to FA and azaC were analyzed. Unlike the *mfd* mutant, the *dksA* and *greA* mutants exhibited no UV sensitivity (Fig. 4J). The *greA* mutant was not sensitive to FA (Fig. 4H). However, the *dksA* mutant exhibited a slight but significant sensitivity to FA (Fig. 4H), implying a certain effect of DksA on the stability of transcription elongation complexes trapped by DPCs. The *greA* and *dksA* mutants were not sensitive to azaC (Fig. 4I).

BER mutants are slightly sensitive to FA, and DNA glycosylases alleviate azaC toxicity to cells. In BER, aberrant bases with minor modifications are removed by DNA glycosylases, and the resulting abasic sites (or nicked abasic sites) are processed by apurinic/apyrimidinic (AP) endonucleases. In *E. coli*, endonucleases III (*nth*) and VIII (*nei*) and formamidopyrimidine glycosylase (*fpg*) account for the major DNA glycosylase activity for oxidized or fragmented pyrimidines (*nth* and *nei*) and purines (*fpg*) (77). Exonuclease III (*xth*) and endonuclease IV (*nfo*) account for the major AP endonuclease activity (16). To clarify whether BER contributes to the repair of DPCs, the sensitivities of glycosylase and AP endonuclease mutants to FA and azaC were assayed. With FA treatment, the *nei nth fpg* triple mutant and the *xth nfo* double mutant exhibited a slight but significant FA sensitivity (Fig. 5A and C). The *fpg* and *nei nth* mutants were virtually insensitive to FA (Fig. 5A). Thus, elimination of three major DNA glycosylases (or AP lyase activity associated with DNA glycosylases) or two major AP endonucleases confers some FA sensitivity on cells. It remains to be seen whether these BER enzymes are involved in the repair of the cryptic base damage induced by FA (i.e., minor base modifications) or FA-induced DPCs per se, although the latter seems unlikely. However, the relative weak sensitivities of the *nei nth fpg* triple mutant and the *xth nfo* double mutant indicate that BER plays at most a minor role in cell survival following FA treatment. Surprisingly, the *nei nth fpg* triple mutant exhibited unexpected strong sensitivity to azaC (Fig. 5B). However, the azaC sensitivity of the triple mutant was not as high as that of the hypersensitive *recA* mutant. The *fpg* single and *nei nth* double mutants were virtually insensitive to azaC. Also, the *xth nfo* double mutant was not sensitive to azaC (Fig. 5D). These results imply that Nei/Nth and Fpg glycosylases complement each other in vivo and remove lethal or potentially lethal DNA damage and that Xth and Nfo that generally act following glycosylases in BER are dispensable in mitigating azaC toxicity to cells (see Discussion).

***topA* mutants are slightly sensitive to FA.** Not much is known about whether DNA topoisomerases participate in DNA repair in *E. coli* (39, 69). *E. coli* has two type I topoisomerases (Topo I and III) and two type II topoisomerases (gyrase and Topo IV), and only Topo III is dispensable for cell growth (9). To obtain insight into the role of topoisomerases in the repair/tolerance of DPCs, we used two Topo mutants (Table 1). RFM445 contains mutations (*gyrB221* and *gyrB203*) in the *gyrB* gene encoding the gyrase subunit B. The mutations confer coumermycin resistance (Cou^r) (*gyrB221*) and cause temperature sensitivity (*gyrB203*) (17, 45). The gyrase comprising GyrA (wt) and mutant GyrB (*gyrB203*) has an activity less than 1% of the normal enzyme at 42°C (45). Thus, the *gyrB203* mutation causes partial inactivation of gyrase at 37°C, which was substantiated by the slow-growing phenotype of RFM445 relative to the wt at 37°C (see Fig. S1A in the supplemental material). RFM475 contains the deletion of the *topA* gene encoding Topo I, together with the mutations *gyrB221* and *gyrB203*. The *gyrB203* mutation compensates for the lack of DNA relaxing activity associated with the *topA* mutation (15, 56). Although the *gyrB203* allele retains minimum activity to allow cell growth at 37°C, it regains gyrase activity at 30°C and is no longer sufficient as a compensatory mutation, rendering the *gyrB203 topA* mutant cold sensitive (17). This phenotype was confirmed in the present study (see Fig. S1B in the supplemental material). Keeping in mind the phenotypes described above, we assessed the sensitivity of RFM445 [*gyrB*(Ts)] and RFM475 [*gyrB*(Ts) *topA*] to FA and azaC at 37°C. The *gyrB*(Ts) mutant was sensitive to neither FA nor azaC (Fig. 5E and F). However, the *gyrB*(Ts) *topA* mutant was slightly sensitive to FA (Fig. 5E), suggesting a role of Topo I in the processing of FA-induced DPCs. The *gyrB*(Ts) *topA* mutant was not sensitive to azaC (Fig. 5F).

General characteristics of genes that alleviate the detrimental effect of DPCs. Figure 6 shows the summary of the sensitivities to the DPC-inducing agents (FA and azaC) displayed by the mutants, including those deficient in damage tolerance (HR, RR, and TLS), excision repair (NER and BER), and miscellaneous aspects of DNA transactions. The data were derived from those shown in Fig. 1 to 5 and Fig. S2 in the supplemental material. The fold increases in the sensitivities of mutants relative to the corresponding wt were calculated at the FA and azaC concentrations indicated in Fig. 6. With hypersensitive mutants, the survival data at lower concentrations were used for calculation (Fig. 6). Although the data in Fig. 6

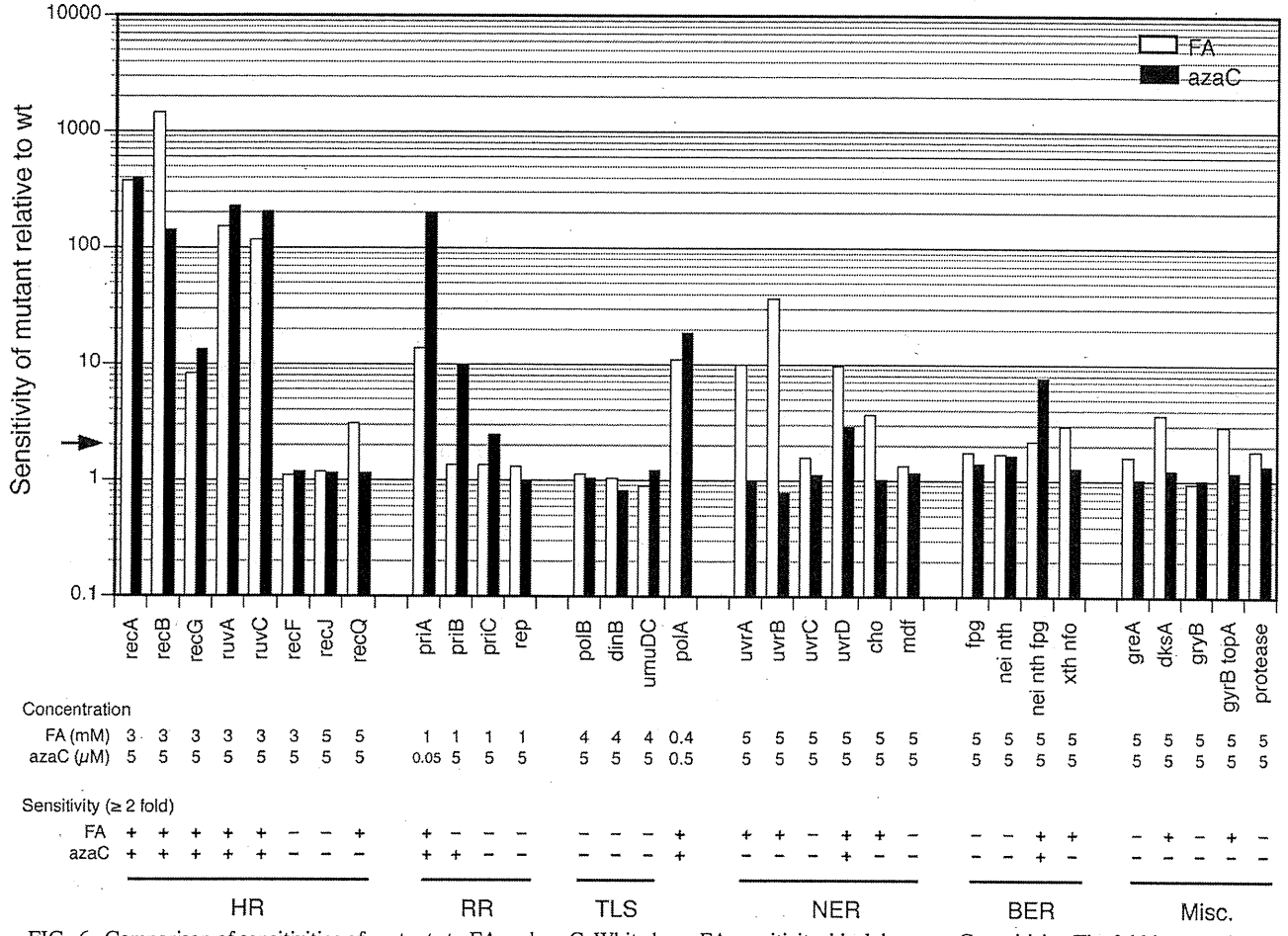

FIG. 6. Comparison of sensitivities of mutants to FA and azaC. White bars, FA sensitivity; black bars, azaC sensitivity. The fold increase in the sensitivity of a mutant relative to the corresponding wt was calculated at the indicated concentrations of FA and azaC. Note that with hypersensitive mutants, the survival data at lower concentrations were used for calculation, since survival data at standard FA and azaC concentrations were not available. The survival data were derived from those shown in Fig. 1 to 5 and Fig. S2 in the supplemental material. The mutants which exhibited more than twofold-greater sensitivities (indicated with an arrow) are indicated by plus signs, and those which did not are indicated by minus signs below the graph. Genes are categorized according to damage tolerance (HR, RR, and TLS), excision repair (NER and BER), and miscellaneous (Misc.) mechanisms. The data under the protease are for the mutant deficient in all cytosolic ATP-dependent proteases (*lon*, *clpAP*, *clpXP*, and *hslVU* with a *sulA* background) that was shown not to be involved in DPC processing prior to NER (51).

allow only semiquantitative analysis, they reveal general aspects of genes that alleviate the detrimental effect of DPCs (tentative threshold for significance set as a twofold increase in sensitivity). First of all, the damage tolerance mechanism involving HR and subsequent RR provides the most effective means for cell survival against DPCs. TLS does not serve as an alternative damage tolerance mechanism for DPCs so far as cell survival is concerned. Elimination of DPCs from the genome relies primarily on NER, which provides a second and moderately effective means for cell survival against DPCs. Interestingly, Cho rather than UvrC seems to be an effective nuclease for the NER of DPCs. The role of DNA polymerase I (*polA*) in both HR and NER has been confirmed. Together with the genes responsible for HR, RR, and NER, the mutation of genes involved in several aspects of DNA repair or transactions (i.e., *recQ*, *nei nth fpg*, *xth nfo*, *dksA*, and *topA*) rendered cell sensitivities to FA to increase by twofold or slightly more. Except for the *nei nth fpg* triple mutant, this was characteristic of FA but not azaC, probably reflecting the unique complexity of DPCs induced by FA or other FA-induced cryptic base modifications. UvrD may have a role outside NER, since the *uvrD* mutation conferred a threefold increase in azaC sensitivity on cells. The triple mutant of DNA glycosylases (*nei nth fpg*) exhibited weak and moderate sensitivities to FA and azaC, respectively. The moderate azaC sensitivity of the mutant may be related to the removal of azaC incorporated into DNA or related degradation products.

We measured the doubling time of strains used in this study to see whether their growth properties had something to do with FA and azaC sensitivities. Among the strains used, the following strains grew poorly and had more than 1.2-fold-greater doubling time than the wt: *priA*, *recB*, *nei nth*, *nei nth fpg*, *polA*, *polA dinB polB umuDC*, *gyrB*(Ts), and *gyrB*(Ts) *topA* (see Table S1 in the supplemental material). The poorly growing strains exhibited various degrees of FA and azaC sensitivities (see Table S1 in the supplemental material). The mutants

such as *priA*, *recB*, and *polA* mutants that grow poorly and exhibit low viability under normal conditions may be sensitive to DNA damage for indirect as well as direct reasons.

DISCUSSION

In the present study, we examined the FA and azaC sensitivities of a panel of *E. coli* repair mutants to extend our understanding of the repair and tolerance mechanisms of DPCs. The present results have confirmed that HR-dependent damage tolerance and NER-dependent damage repair mechanisms play pivotal roles in cell survival when the genome becomes burdened with DPCs, with the former making a more significant and crucial contribution. The RR following the HR of DPCs relies on the PriA-dependent mechanisms, where the PriA-PriB pathway likely contributes to RR more than the PriA-PriC pathway does, although the two pathways can compensate for each other to a significant degree when one is compromised. Neither TLS nor TCR, a subpathway of NER, is involved in the damage tolerance and repair mechanisms of DPCs.

Recently, the DNA damage response to FA was assessed using chicken DT40 cells with targeted mutations in various DNA repair genes (59). The DT40 cells deficient in HR and TLS were hypersensitive to FA, and those deficient in NER and BER were moderately to slightly sensitive. Thus, the roles of HR, NER, and BER in DPC tolerance and repair are essentially parallel in *E. coli* and DT40 cells, but there is a sharp contrast between the involvement of TLS in *E. coli* and DT40 cells in terms of DPC tolerance. The TLS mutants of DT40 examined for FA sensitivity were REV1, REV3, and RAD18 (59). REV3 is the catalytic subunit of Pol ζ, and REV1 has dCMP transferase activity and may serve as a scaffolding protein which associates with TLS polymerases. RAD18, together with RAD6, forms an E2-E3 complex that monoubiquitinates PCNA, likely assisting the switch from replicative to bypass polymerases at the lesion (22). We suspect it is very unlikely that prokaryotic and eukaryotic TLS polymerases directly bypass DPCs in view of the enormous steric hindrance conferred by DPCs, raising the possibility that TLS polymerases have a role outside the direct bypass of DPCs. Furthermore, direct damage bypass is not relevant when DPCs impede the progression of the replicative helicase working ahead of polymerase. It has been suggested that *E. coli* TLS polymerases are involved in RR (12) or template switching after regression of the stalled fork (23), allowing indirect damage bypass. However, inactivation of all of the TLS polymerases (encoded by *polB*, *dinB*, and *umuDC*) in *E. coli* had no impact on cell survival to FA and azaC (Fig. 3B and D), ruling out this possibility. Functions of TLS polymerases in eukaryotic cells have been suggested to be not only in TLS but also in HR (reviewed in reference 22). Thus, the FA sensitivities of DT40 REV1 and REV3 mutants may be related to HR. It will be interesting to elucidate whether TLS mutants of other eukaryotic cells, such as yeast and mammalian cells, share a similar sensitivity to DPC-inducing agents, as observed in DT40 cells.

In this study, it was suggested that Cho, rather than UvrC, is an effective nuclease for the NER of DPCs, although both *cho* and *uvrC* single mutants were less FA sensitive than the *uvrA*, *uvrB*, and *uvrD* mutants (Fig. 4A and E). Cho has been implicated in NER and has unique properties, as follows (48). Cho shares significant homology with the N-terminal half of UvrC, which is responsible for incisions at the 3′ side of the lesion. The *cho* mutation does not confer UV sensitivity on cells, but it does slightly increase the sensitivity of the *uvrC* mutant, although we did not observe such an increase in this study (Fig. 4G). Some synthetic bulky lesions that are poorly incised by UvrC are efficiently incised by Cho in vitro. Cho produces only 3′ incisions, and the incision site is four nucleotides further away from the lesion than that of UvrC. Thus, unusually bulky lesions might sterically hinder access by UvrC, but not Cho, to produce the 3′ incision (48, 74). Accordingly, Cho may be able to incise DNA on the 3′ side of DPCs containing proteins of up to a certain size. The 5′ side of DPC would be incised by the C-terminal half of UvrC, which is sufficient to produce the second incision. Interestingly, the additional *uvrC* mutation in the *cho* mutant did not enhance the FA sensitivity (Fig. 4E). A possible interpretation of this result is that UvrC and Cho collaborate with each other in vivo and expand the capacity of NER for DPCs. However, the present result argues against this mechanism, since the *cho* single mutation conferred greater FA sensitivity on cells than the *uvrC* single mutation did, suggesting that the single 3′ incision of DPCs by Cho, but not the 3′ and 5′ dual incisions by UvrC or the combination of Cho and UvrC, is the dominant repair pathway of DPCs. Further biochemical and in vivo studies are necessary to clarify whether this is the case.

Together with mutations in the genes responsible for HR, RR, and NER, we found that those involved in several aspects of DNA repair or transactions conferred cells' slight but significant sensitivity to FA and/or azaC. UvrD is a highly conserved 3′ to 5′ helicase involved in NER and mismatch repair (43, 73). The *uvrD* mutant was sensitive to FA (Fig. 4E), in keeping with our previous result that FA-induced DPCs containing small cross-linked proteins were repaired by NER in vivo (51). In addition, the *uvrD* mutant showed a slight but significant sensitivity to azaC compared to wt and other *uvr* mutant cells (Fig. 4E and F). In view of the size limit of cross-linked proteins amenable to NER (12 to 14 kDa), the DPC containing 53-kDa Dcm induced by azaC should be processed by HR. It has been proposed that UvrD prevents the unnecessary recombination by dismantling the RecA-DNA complex, which may be lethal (18, 75). Accordingly, the UvrD helicase may prevent a deleterious recombination at the replication fork arrested by DPC and thereby mitigate the lethal effect of DPC. However, the contribution of this mechanism to cell survival seems to be moderate, as judged from the mild sensitivity of the *uvrD* mutant to azaC.

In *E. coli*, the supercoiling of chromosomes is regulated by DNA topoisomerases. DNA gyrase (*gyrA* and *gyrB*) introduces negative supercoils, whereas Topo I (*topA*) and Topo IV (*parC* and *parE*) remove excess negative supercoils (9). The *topA* mutant is sensitive to UV light and methanesulfonate (69). Furthermore, topoisomerases are implicated in the HR of DNA damage (39). The *gyrB*(Ts) mutant partially defective in DNA gyrase was sensitive to neither FA nor azaC (Fig. 5E and F). However, the mutation in the *topA* gene encoding Topo I rendered cells slightly sensitive to FA but not azaC (Fig. 5E and F). The *topA* mutant used here carried an additional *gyrB*(Ts) mutation as an inevitable compensatory mutation, but

the *gyrB*(Ts) mutation alone had no impact on cell survival following FA treatment (Fig. 5E). The FA sensitivity of the *gyrB*(Ts) *topA* mutant is not due to redundant activity, since Topo I (*topA*) and DNA gyrase (*gyrB*) introduce opposite polarities of supercoils. In the previous study, we demonstrated that FA induces two types of DPCs. One contains proteins covalently trapped on the DNA strand. The other contains proteins covalently bridging two duplex DNA strands. The former is common for FA- and azaC-induced DPCs, but the latter is characteristic of FA-induced DPCs. FA also induces direct interstrand cross-links between DNA bases within a duplex (31). Although similar interstrand cross-links mediated by protein have not been identified so far in FA-treated cells, such cross-links may also be formed by FA. Thus, it is tempting to speculate that the direct or protein-mediated DNA-DNA cross-links may hamper the topological changes of DNA catalyzed by Topo I in HR or NER. The mutants that exhibited damage sensitivity similar to that of *topA* (i.e., *recQ*, *xth nfo*, and *dksA* mutants) may also be defective in the processing of such DNA-DNA cross-links.

Finally, we found that the *nei nth fpg* triple mutant, but not the *fpg* single and *nei nth* double mutants, was moderately sensitive to azaC (Fig. 5B). Curiously, *xth* and *nfo* that act following glycosylases in BER were dispensable in mitigating azaC toxicity (Fig. 5D). These results at least point to the fact that Nei/Nth and Fpg glycosylases complement each other in vivo and remove lethal or potentially lethal DNA damage, although it is not clear why Xth and Nfo are not involved in the subsequent step of BER. In view of the restricted space of the active site pocket of DNA glycosylases that accommodate only minor base modifications (28), it is very unlikely that Nei, Nth, and Fpg recognize extremely large DPCs as damage and excise them from DNA. There seem to be three mechanisms that might account for the azaC sensitivity of the *nei nth fpg* triple mutant. First, Nei/Nth and Fpg recognize 5-azacytosine (base moiety of azaC) as damage and excise it from DNA. If true, 5-azacytosine left unrepaired in the triple mutant will covalently trap Dcm and thereby increase the azaC sensitivity of the cell. Second, Nei/Nth and Fpg are involved in the repair of the degradation products of 5-azacytosine, since 5-azacytosine is fairy unstable and slowly hydrolyzes to ring fragmentation products (42). Like other ring fragmentation products of DNA bases (32, 33), those of 5-azacytosine left unrepaired in the triple mutant will arrest DNA replication and thereby increase the azaC sensitivity of the cell. Third, in the triple mutant, the AP lyase of Nei, Nth, and Fpg is also inactivated, pointing to a mechanism associated with the reduced AP lyase activity of cells. Analyses of the formation and repair of 5-azacytosine, degradation products, and Dcm-DPCs in vivo, together with those of the activity of Nei, Nth, and Fpg to 5-azacytosine and degradation products in vitro, will shed light on the molecular mechanism of azaC toxicity associated with the defect in DNA glycosylases.

ACKNOWLEDGMENTS

We are grateful to M. Bichara (CNRS), M. Drolet (Université de Montréal), N. Goosen (Leiden University), T. Hishida (Osaka University), H. Iwasaki (Yokohama City University), R. G. Lloyd (University of Nottingham), M. G. Marinus (University of Massachusetts), S. J. Sandler (University of Massachusetts), R. Woodgate (NICHD/NIH), S. Yonei (Kyoto University), S. S. Wallace (University of Vermont), the Coli Genetic Stock Center (http://cgsc.biology.yale.edu/), and the National BioResource Project (http://www.nbrp.jp/) for the generous gifts of *E. coli* strains and plasmids.

This work was supported in part by Grants-in-Aid for Scientific Research from the Japan Society for the Promotion of Science (H.I. and T.N.) and the Support Program for Improving Graduate School Education from the Japan Society for the Promotion of Science (A.M.H.S.).

REFERENCES

1. **Akasaka, S., and K. Yamamoto.** 1991. Construction of *Escherichia coli* K12 *phr* deletion and insertion mutants by gene replacement. Mutat. Res. **254:**27–35.
2. **Baker, D. J., G. Wuenschell, L. Xia, J. Termini, S. E. Bates, A. D. Riggs, and T. R. O'Connor.** 2007. Nucleotide excision repair eliminates unique DNA-protein cross-links from mammalian cells. J. Biol. Chem. **282:**22592–22604.
3. **Barker, S., M. Weinfeld, and D. Murray.** 2005. DNA-protein crosslinks: their induction, repair, and biological consequences. Mutat. Res. **589:**111–135.
4. **Beckerbauer, L., J. J. Tepe, J. Cullison, R. Reeves, and R. M. Williams.** 2000. FR900482 class of anti-tumor drugs cross-links oncoprotein HMG I/Y to DNA *in vivo*. Chem. Biol. **7:**805–812.
5. **Bhagwat, A. S., and R. J. Roberts.** 1987. Genetic analysis of the 5-azacytidine sensitivity of *Escherichia coli* K-12. J. Bacteriol. **169:**1537–1546.
6. **Bichara, M., I. Pinet, M. Origas, and R. P. Fuchs.** 2006. Inactivation of *recG* stimulates the RecF pathway during lesion-induced recombination in *E. coli*. DNA Repair **5:**129–137.
7. **Blaisdell, J. O., Z. Hatahet, and S. S. Wallace.** 1999. A novel role for *Escherichia coli* endonuclease VIII in prevention of spontaneous G→T transversions. J. Bacteriol. **181:**6396–6402.
8. **Boiteux, S., and O. Huisman.** 1989. Isolation of a formamidopyrimidine-DNA glycosylase (*fpg*) mutant of *Escherichia coli* K12. Mol. Gen. Genet. **215:**300–305.
9. **Champoux, J. J.** 2001. DNA topoisomerases: structure, function, and mechanism. Annu. Rev. Biochem. **70:**369–413.
10. **Chichiarelli, S., S. Coppari, C. Turano, M. Eufemi, F. Altieri, and A. Ferraro.** 2002. Immunoprecipitation of DNA-protein complexes cross-linked by *cis*-diamminedichloroplatinum. Anal. Biochem. **302:**224–229.
11. **Courcelle, C. T., J. J. Belle, and J. Courcelle.** 2005. Nucleotide excision repair or polymerase V-mediated lesion bypass can act to restore UV-arrested replication forks in *Escherichia coli*. J. Bacteriol. **187:**6953–6961.
12. **Courcelle, C. T., K. H. Chow, A. Casey, and J. Courcelle.** 2006. Nascent DNA processing by RecJ favors lesion repair over translesion synthesis at arrested replication forks in *Escherichia coli*. Proc. Natl. Acad. Sci. USA **103:**9154–9159.
13. **Cunningham, R. P., S. M. Saporito, S. G. Spitzer, and B. Weiss.** 1986. Endonuclease IV (*nfo*) mutant of *Escherichia coli*. J. Bacteriol. **168:**1120–1127.
14. **Datsenko, K. A., and B. L. Wanner.** 2000. One-step inactivation of chromosomal genes in *Escherichia coli* K-12 using PCR products. Proc. Natl. Acad. Sci. USA **97:**6640–6645.
15. **DiNardo, S., K. A. Voelkel, R. Sternglanz, A. E. Reynolds, and A. Wright.** 1982. *Escherichia coli* DNA topoisomerase I mutants have compensatory mutations in DNA gyrase genes. Cell **31:**43–51.
16. **Doetsch, P. W., and R. P. Cunningham.** 1990. The enzymology of apurinic/apyrimidinic endonucleases. Mutat. Res. **236:**173–201.
17. **Drolet, M., P. Phoenix, R. Menzel, E. Masse, L. F. Liu, and R. J. Crouch.** 1995. Overexpression of RNase H partially complements the growth defect of an *Escherichia coli* Δ*topA* mutant: R-loop formation is a major problem in the absence of DNA topoisomerase I. Proc. Natl. Acad. Sci. USA **92:**3526–3530.
18. **Florés, M. J., N. Sanchez, and B. Michel.** 2005. A fork-clearing role for UvrD. Mol. Microbiol. **57:**1664–1675.
19. **Frank, E. G., M. Gonzalez, D. G. Ennis, A. S. Levine, and R. Woodgate.** 1996. In vivo stability of the Umu mutagenesis proteins: a major role for RecA. J. Bacteriol. **178:**3550–3556.
20. **Friedberg, E. C., G. C. Walker, W. Siede, R. D. Wood, R. A. Schultzs, and T. Ellenberger.** 2006. DNA repair and mutagenesis, 2nd ed. American Society for Microbiology, Washington, DC.
21. **Friedman, S.** 1985. The irreversible binding of azacytosine-containing DNA fragments to bacterial DNA(cytosine-5)methyltransferases. J. Biol. Chem. **260:**5698–5705.
22. **Gan, G. N., J. P. Wittschieben, B. O. Wittschieben, and R. D. Wood.** 2008. DNA polymerase zeta (pol ζ) in higher eukaryotes. Cell Res. **18:**174–183.
23. **Goodman, M. F.** 2002. Error-prone repair DNA polymerases in prokaryotes and eukaryotes. Annu. Rev. Biochem. **71:**17–50.
24. **Heller, R. C., and K. J. Marians.** 2005. Unwinding of the nascent lagging strand by Rep and PriA enables the direct restart of stalled replication forks. J. Biol. Chem. **280:**34143–34151.
25. **Higgins, N. P., K. Kato, and B. Strauss.** 1976. A model for replication repair in mammalian cells. J. Mol. Biol. **101:**417–425.
26. **Hishida, T., Y. W. Han, T. Shibata, Y. Kubota, Y. Ishino, H. Iwasaki, and H. Shinagawa.** 2004. Role of the *Escherichia coli* RecQ DNA helicase in SOS signaling and genome stabilization at stalled replication forks. Genes Dev. **18:**1886–1897.

27. **Hishida, T., H. Iwasaki, K. Ishioka, and H. Shinagawa.** 1996. Molecular analysis of the *Pseudomonas aeruginosa* genes, *ruvA*, *ruvB* and *ruvC*, involved in processing of homologous recombination intermediates. Gene **182:**63–70.
28. **Hitomi, K., S. Iwai, and J. A. Tainer.** 2007. The intricate structural chemistry of base excision repair machinery: implications for DNA damage recognition, removal, and repair. DNA Repair **6:**410–428.
29. **Howard-Flanders, P., R. P. Boyce, and L. Theriot.** 1966. Three loci in *Escherichia coli* K-12 that control the excision of pyrimidine dimers and certain other mutagen products from DNA. Genetics **53:**1119–1136.
30. **Howard-Flanders, P., and L. Theriot.** 1966. Mutants of *Escherichia coli* K-12 defective in DNA repair and in genetic recombination. Genetics **53:**1137–1150.
31. **Huang, H., and P. B. Hopkins.** 1993. DNA interstrand cross-linking by formaldehyde: nucleotide sequence preference and covalent structure of the predominant cross-link formed in synthetic oligonucleotides. J. Am. Chem. Soc. **115:**9402–9408.
32. **Ide, H., Y. W. Kow, and S. S. Wallace.** 1985. Thymine glycols and urea residues in M13 DNA constitute replicative blocks *in vitro*. Nucleic Acids Res. **13:**8035–8052.
33. **Ide, H., L. A. Petrullo, Z. Hatahet, and S. S. Wallace.** 1991. Processing of DNA base damage by DNA polymerases. Dihydrothymine and β-ureidoisobutyric acid as models for instructive and noninstructive lesions. J. Biol. Chem. **266:**1469–1477.
34. **Ishioka, K., A. Fukuoh, H. Iwasaki, A. Nakata, and H. Shinagawa.** 1998. Abortive recombination in *Escherichia coli ruv* mutants blocks chromosome partitioning. Genes Cells **3:**209–220.
35. **Joyce, C. M., and N. D. Grindley.** 1984. Method for determining whether a gene of *Escherichia coli* is essential: application to the *polA* gene. J. Bacteriol. **158:**636–643.
36. **Kogoma, T., G. W. Cadwell, K. G. Barnard, and T. Asai.** 1996. The DNA replication priming protein, PriA, is required for homologous recombination and double-strand break repair. J. Bacteriol. **178:**1258–1264.
37. **Kosa, J. L., Z. Z. Zdraveski, S. Currier, M. G. Marinus, and J. M. Essigmann.** 2004. RecN and RecG are required for *Escherichia coli* survival of bleomycin-induced damage. Mutat. Res. **554:**149–157.
38. **Kuo, H. K., J. D. Griffith, and K. N. Kreuzer.** 2007. 5-Azacytidine induced methyltransferase-DNA adducts block DNA replication *in vivo*. Cancer Res. **67:**8248–8254.
39. **Kuzminov, A.** 1999. Recombinational repair of DNA damage in *Escherichia coli* and bacteriophage λ. Microbiol. Mol. Biol. Rev. **63:**751–813.
40. **Lal, D., S. Som, and S. Friedman.** 1988. Survival and mutagenic effects of 5-azacytidine in *Escherichia coli*. Mutat. Res. **193:**229–236.
41. **Liu, J., L. Xu, S. J. Sandler, and K. J. Marians.** 1999. Replication fork assembly at recombination intermediates is required for bacterial growth. Proc. Natl. Acad. Sci. USA **96:**3552–3555.
42. **Liu, Z., G. Marcucci, J. C. Byrd, M. Grever, J. Xiao, and K. K. Chan.** 2006. Characterization of decomposition products and preclinical and low dose clinical pharmacokinetics of decitabine (5-aza-2′-deoxycytidine) by a new liquid chromatography/tandem mass spectrometry quantification method. Rapid Commun. Mass Spectrom. **20:**1117–1126.
43. **Matson, S. W., and A. B. Robertson.** 2006. The UvrD helicase and its modulation by the mismatch repair protein MutL. Nucleic Acids Res. **34:**4089–4097.
44. **Matsumoto, A., and P. C. Hanawalt.** 2000. Histone H3 and heat shock protein GRP78 are selectively cross-linked to DNA by photoactivated gilvocarcin V in human fibroblasts. Cancer Res. **60:**3921–3926.
45. **Menzel, R., and M. Gellert.** 1983. Regulation of the genes for *E. coli* DNA gyrase: homeostatic control of DNA supercoiling. Cell **34:**105–113.
46. **Minko, I. G., A. J. Kurtz, D. L. Croteau, B. Van Houten, T. M. Harris, and R. S. Lloyd.** 2005. Initiation of repair of DNA-polypeptide cross-links by the UvrABC nuclease. Biochemistry **44:**3000–3009.
47. **Minko, I. G., Y. Zou, and R. S. Lloyd.** 2002. Incision of DNA-protein crosslinks by UvrABC nuclease suggests a potential repair pathway involving nucleotide excision repair. Proc. Natl. Acad. Sci. USA **99:**1905–1909.
48. **Moolenaar, G. F., S. van Rossum-Fikkert, M. van Kesteren, and N. Goosen.** 2002. Cho, a second endonuclease involved in *Escherichia coli* nucleotide excision repair. Proc. Natl. Acad. Sci. USA **99:**1467–1472.
49. **Nakano, T., K. Asagoshi, H. Terato, T. Suzuki, and H. Ide.** 2005. Assessment of the genotoxic potential of nitric oxide-induced guanine lesions by in vitro reactions with *Escherichia coli* DNA polymerase I. Mutagenesis **20:**209–216.
50. **Nakano, T., A. Katafuchi, R. Shimizu, H. Terato, T. Suzuki, H. Tauchi, K. Makino, M. Skorvaga, B. Van Houten, and H. Ide.** 2005. Repair activity of base and nucleotide excision repair enzymes for guanine lesions induced by nitrosative stress. Nucleic Acids Res. **33:**2181–2191.
51. **Nakano, T., S. Morishita, A. Katafuchi, M. Matsubara, Y. Horikawa, H. Terato, A. M. Salem, S. Izumi, S. P. Pack, K. Makino, and H. Ide.** 2007. Nucleotide excision repair and homologous recombination systems commit differentially to the repair of DNA-protein crosslinks. Mol. Cell **28:**147–158.
52. **Nakano, T., H. Terato, K. Asagoshi, A. Masaoka, M. Mukuta, Y. Ohyama, T. Suzuki, K. Makino, and H. Ide.** 2003. DNA-protein cross-link formation mediated by oxanine. A novel genotoxic mechanism of nitric oxide-induced DNA damage. J. Biol. Chem. **278:**25264–25272.
53. **Nakayama, K., K. Kusano, N. Irino, and H. Nakayama.** 1994. Thymine starvation-induced structural changes in *Escherichia coli* DNA. Detection by pulsed field gel electrophoresis and evidence for involvement of homologous recombination. J. Mol. Biol. **243:**611–620.
54. **Nishioka, H.** 1973. Lethal and mutagenic action of formaldehyde in Hcr^+ and Hcr^- strains of *Escherichia coli*. Mutat. Res. **17:**261–265.
55. **Nohmi, T.** 2006. Environmental stress and lesion-bypass DNA polymerases. Annu. Rev. Microbiol. **60:**231–253.
56. **Pruss, G. J., S. H. Manes, and K. Drlica.** 1982. *Escherichia coli* DNA topoisomerase I mutants: increased supercoiling is corrected by mutations near gyrase genes. Cell **31:**35–42.
57. **Rangarajan, S., R. Woodgate, and M. F. Goodman.** 1999. A phenotype for enigmatic DNA polymerase II: a pivotal role for pol II in replication restart in UV-irradiated *Escherichia coli*. Proc. Natl. Acad. Sci. USA **96:**9224–9229.
58. **Reardon, J. T., and A. Sancar.** 2006. Repair of DNA-polypeptide crosslinks by human excision nuclease. Proc. Natl. Acad. Sci. USA **103:**4056–4061.
59. **Ridpath, J. R., A. Nakamura, K. Tano, A. M. Luke, E. Sonoda, H. Arakawa, J. M. Buerstedde, D. A. Gillespie, J. E. Sale, M. Yamazoe, D. K. Bishop, M. Takata, S. Takeda, M. Watanabe, J. A. Swenberg, and J. Nakamura.** 2007. Cells deficient in the FANC/BRCA pathway are hypersensitive to plasma levels of formaldehyde. Cancer Res. **67:**11117–11122.
60. **Saito, Y., F. Uraki, S. Nakajima, A. Asaeda, K. Ono, K. Kubo, and K. Yamamoto.** 1997. Characterization of endonuclease III (*nth*) and endonuclease VIII (*nei*) mutants of *Escherichia coli* K-12. J. Bacteriol. **179:**3783–3785.
61. **Saka, K., M. Tadenuma, S. Nakade, N. Tanaka, H. Sugawara, K. Nishikawa, N. Ichiyoshi, M. Kitagawa, H. Mori, N. Ogasawara, and A. Nishimura.** 2005. A complete set of *Escherichia coli* open reading frames in mobile plasmids facilitating genetic studies. DNA Res. **12:**63–68.
62. **Samuel, S. K., V. A. Spencer, L. Bajno, J. M. Sun, L. T. Holth, S. Oesterreich, and J. R. Davie.** 1998. *In situ* cross-linking by cisplatin of nuclear matrix-bound transcription factors to nuclear DNA of human breast cancer cells. Cancer Res. **58:**3004–3008.
63. **Sandler, S. J.** 2000. Multiple genetic pathways for restarting DNA replication forks in *Escherichia coli* K-12. Genetics **155:**487–497.
64. **Sandler, S. J., and K. J. Marians.** 2000. Role of PriA in replication fork reactivation in *Escherichia coli*. J. Bacteriol. **182:**9–13.
65. **Santi, D. V., A. Norment, and C. E. Garrett.** 1984. Covalent bond formation between a DNA-cytosine methyltransferase and DNA containing 5-azacytosine. Proc. Natl. Acad. Sci. USA **81:**6993–6997.
66. **Selby, C. P., and A. Sancar.** 1993. Molecular mechanism of transcription-repair coupling. Science **260:**53–58.
67. **Shinagawa, H., H. Iwasaki, Y. Ishino, and A. Nakata.** 1991. SOS-inducible DNA polymerase II of *E. coli* is homologous to replicative DNA polymerase of eukaryotes. Biochimie **73:**433–435.
68. **Singer, M., T. A. Baker, G. Schnitzler, S. M. Deischel, M. Goel, W. Dove, K. J. Jaacks, A. D. Grossman, J. W. Erickson, and C. A. Gross.** 1989. A collection of strains containing genetically linked alternating antibiotic resistance elements for genetic mapping of *Escherichia coli*. Microbiol. Rev. **53:**1–24.
69. **Sternglanz, R., S. DiNardo, K. A. Voelkel, Y. Nishimura, Y. Hirota, K. Becherer, L. Zumstein, and J. C. Wang.** 1981. Mutations in the gene coding for *Escherichia coli* DNA topoisomerase I affect transcription and transposition. Proc. Natl. Acad. Sci. USA **78:**2747–2751.
70. **Takahashi, K., T. Morita, and Y. Kawazoe.** 1985. Mutagenic characteristics of formaldehyde on bacterial systems. Mutat. Res. **156:**153–161.
71. **Takahashi, N. K., K. Kusano, T. Yokochi, Y. Kitamura, H. Yoshikura, and I. Kobayashi.** 1993. Genetic analysis of double-strand break repair in *Escherichia coli*. J. Bacteriol. **175:**5176–5185.
72. **Trautinger, B. W., R. P. Jaktaji, E. Rusakova, and R. G. Lloyd.** 2005. RNA polymerase modulators and DNA repair activities resolve conflicts between DNA replication and transcription. Mol. Cell **19:**247–258.
73. **Truglio, J. J., D. L. Croteau, B. Van Houten, and C. Kisker.** 2006. Prokaryotic nucleotide excision repair: the UvrABC system. Chem. Rev. **106:**233–252.
74. **Van Houten, B., J. A. Eisen, and P. C. Hanawalt.** 2002. A cut above: discovery of an alternative excision repair pathway in bacteria. Proc. Natl. Acad. Sci. USA **99:**2581–2583.
75. **Veaute, X., S. Delmas, M. Selva, J. Jeusset, E. Le Cam, I. Matic, F. Fabre, and M. A. Petit.** 2005. UvrD helicase, unlike Rep helicase, dismantles RecA nucleoprotein filaments in *Escherichia coli*. EMBO J. **24:**180–189.
76. **Wagner, J., and T. Nohmi.** 2000. *Escherichia coli* DNA polymerase IV mutator activity: genetic requirements and mutational specificity. J. Bacteriol. **182:**4587–4595.
77. **Wallace, S. S.** 2002. Biological consequences of free radical-damaged DNA bases. Free Radic. Biol. Med. **33:**1–14.
78. **Woodgate, R.** 1992. Construction of a *umuDC* operon substitution mutation in *Escherichia coli*. Mutat. Res. **281:**221–225.
79. **Yamamoto, K., M. Satake, and H. Shinagawa.** 1984. A multicopy *phr*-plasmid increases the ultraviolet resistance of a *recA* strain of *Escherichia coli*. Mutat. Res. **131:**11–18.

THE JOURNAL OF BIOLOGICAL CHEMISTRY VOL. 284, NO. 38, pp. 25585–25592, September 18, 2009

Translesional DNA Synthesis through a C8-Guanyl Adduct of 2-Amino-1-methyl-6-phenylimidazo[4,5-*b*]pyridine (PhIP) *in Vitro*

REV1 INSERTS dC OPPOSITE THE LESION, AND DNA POLYMERASE κ POTENTIALLY CATALYZES EXTENSION REACTION FROM THE 3′-dC TERMINUS[*][S]

Received for publication, June 25, 2009, and in revised form, July 16, 2009 Published, JBC Papers in Press, July 23, 2009, DOI 10.1074/jbc.M109.037259

Hirokazu Fukuda[‡], Takeji Takamura-Enya[§], Yuji Masuda[¶], Takehiko Nohmi[‖], Chiho Seki[‡], Kenji Kamiya[¶], Takashi Sugimura[‡], Chikahide Masutani[**], Fumio Hanaoka[1], and Hitoshi Nakagama[‡2]**

From the [‡]Biochemistry Division, National Cancer Center Research Institute, 1-1, Tsukiji 5, Chuo-ku, Tokyo 104-0045, the [§]Department of Applied Chemistry, Faculty of Engineering, Kanagawa Institute of Technology, Ogino 1030, Atsugi, Kanagawa 243-0292, the [¶]Department of Experimental Oncology, Research Institute for Radiation Biology and Medicine, Hiroshima University, Kasumi 1-2-3, Minami-ku, Hiroshima, Hiroshima 734-8553, the [‖]Division of Genetics and Mutagenesis, National Institute of Health Sciences, Kamiyoga 1-18-1, Setagaya-ku, Tokyo 158-8501, and the [**]Cellular Biology Laboratory, Graduate School of Frontier Biosciences, Osaka University, Yamada-oka 1-3, Suita, Osaka 565-0871, Japan

2-Amino-1-methyl-6-phenylimidazo[4,5-*b*]pyridine (PhIP) is the most abundant heterocyclic amine in cooked foods, and is both mutagenic and carcinogenic. It has been suspected that the carcinogenicity of PhIP is derived from its ability to form DNA adducts, principally dG-C8-PhIP. To shed further light on the molecular mechanisms underlying the induction of mutations by PhIP, *in vitro* DNA synthesis analyses were carried out using a dG-C8-PhIP-modified oligonucleotide template. In this template, the dG-C8-PhIP adduct was introduced into the second G of the TCC GGG AAC sequence located in the 5′ region. This represents one of the mutation hot spots in the rat *Apc* gene that is targeted by PhIP. Guanine deletions at this site in the *Apc* gene have been found to be preferentially induced by PhIP in rat colon tumors. DNA synthesis with A- or B-family DNA polymerases, such as *Escherichia coli* polymerase (pol) I and human pol δ, was completely blocked at the adducted guanine base. Translesional synthesis polymerases of the Y-family, pol η, pol ι, pol κ, and REV1, were also used for *in vitro* DNA synthesis analyses with the same templates. REV1, pol η, and pol κ were able to insert dCTP opposite dG-C8-PhIP, although the efficiencies for pol η and pol κ were low. pol κ was also able to catalyze the extension reaction from the dC opposite dG-C8-PhIP, during which it often skipped over one dG of the triple dG sequence on the template. This slippage probably leads to the single dG base deletion in colon tumors.

Heterocyclic amines (HCAs)[3] are naturally occurring genotoxic carcinogens produced from cooking meat (1). The initial carcinogenic event induced by HCAs is metabolic activation and subsequent covalent bond formation with DNA (1, 2). 2-Amino-1-methyl-6-phenylimidazo[4,5-*b*]pyridine (PhIP) is the most abundant heterocyclic amine in cooked foods, and was isolated from fried ground beef (3, 4). PhIP possesses both mutagenic and carcinogenic properties (5–8). Epidemiological studies have revealed that a positive correlation exists between PhIP exposure and mammary cancer incidence (9). PhIP induces colon and prostate cancers in male rats and breast cancer in female rats (8, 10).

The incidences of colon, prostate, and breast cancers are steadily increasing in Japan and other countries and this has been found to correlate with a more Westernized lifestyle. Elucidating the molecular mechanisms underlying PhIP-induced mutations is therefore of considerable interest. It is suspected that the carcinogenicity of PhIP is derived from the formation of DNA adducts, principally dG-C8-PhIP (11–14) (see Fig. 1). Studies of the mutation spectrum of PhIP in mammalian cultured cells and transgenic animals have revealed that G to T transversions are predominant and that guanine deletions from G stretches, especially from the 5′-GGGA-3′ sequence, are significant (15–20). Five mutations in the *Apc* gene were detected in four of eight PhIP-induced rat colon tumors, and all of these mutations involved a single base deletion of guanine from 5′-GGGA-3′ (21). These mutation spectra are thought to be influenced by various factors, including the primary structure of the target gene itself, the capacity of translesional DNA polymerases, and the activity level of repair enzymes (1). However, the molecular mechanisms underlying the formation of PhIP-induced mutations are largely unknown.

To shed further light on the molecular processes that underpin the mutations induced by PhIP, we performed *in vitro* DNA synthesis analyses using a dG-C8-PhIP-modified oligonucleotide template. We have recently reported the successful synthesis of oligonucleotides harboring a site-specific PhIP adduct

* This work was supported by Kakenhi Grant 19570144.
[S] The on-line version of this article (available at http://www.jbc.org) contains supplemental Table S1 and Figs. S1–S6.
[1] Present address: Dept. of Life Science, Faculty of Science, Gakushuin University, Mejiro 1-5-1, Toshima-ku, Tokyo 171-8588, Japan.
[2] To whom correspondence should be addressed. Tel.: 81-3-3542-2511; Fax: 81-33542-2530; E-mail: hnakagam@ncc.go.jp.
[3] The abbreviations used are: HCA, heterocyclic amines; PhIP, 2-amino-1-methyl-6-phenylimidazo[4,5-*b*]pyridine; TLS, translesional DNA synthesis; IQ, 2-amino-3-methylimidazo[4,5-*f*]quinoline; pol, DNA polymerase; DTT, dithiothreitol; PCNA, proliferating cell nuclear antigen; PIPES, 1,4-piperazinediethanesulfonic acid.

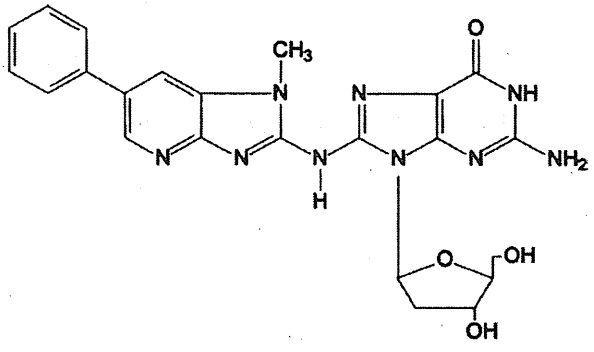

dG-C8-PhIP

FIGURE 1. **Structure of the dG-C8-PhIP adduct.**

(22). In our current study, we used this synthesis method to construct a 32-mer oligonucleotide template containing a 5′-TTCGGGAAC-3′ sequence with different site-specific PhIP adducts. We then utilized the resulting constructs in DNA synthesis analyses to reconstitute the PhIP-induced mutagenesis of the rat *APC* gene. DNA synthesis reactions with A- or B-family DNA polymerases, such as *Escherichia coli* pol I and human pol δ, or translesional synthesis (TLS) polymerases of the Y-family, pol η, pol ι, pol κ, and REV1, were carried out. Kinetic analyses of pol κ and REV1, for which TLS activities at the PhIP adduct were detected, were also performed.

EXPERIMENTAL PROCEDURES

Enzymes and Materials—T4 polynucleotide kinase and T4 DNA ligase were purchased from Toyobo Biochem (Osaka, Japan) and Takara Biotech (Tokyo Japan), respectively. Other materials were obtained from Sigma or Wako (Osaka, Japan).

DNA Polymerases and PCNA—Human recombinant DNA polymerases, pol δ, pol η, pol κ, and REV1, and PCNA were expressed and purified as described previously (23–27). Human DNA polymerase α and DNA polymerase ι were purchased from Chimerx. *E. coli* DNA polymerases I (Takara Biotech) and Klenow Fragment (Takara Biotech), and thermophilic bacterial DNA polymerases, r*Taq* (Toyobo Biochem) and *Tth* (Toyobo Biochem) were used.

Oligonucleotides—The method used to chemically synthesize three 9-mer oligonucleotides, 5′-TCCGGGAAC-3′, containing a PhIP adduct on either the first, second, or third G (p9B, p9C, and p9D, respectively) has been described previously (22). All other synthetic oligonucleotides were synthesized and purified using a reverse-phase cartridge (Operon Biotech Japan (Tokyo, Japan). The 23-mer oligonucleotides: p23a, 5′-TGACTCGTCGTGACTGGGAAAAC-3′, and p23b, 5′-GTCACGACGAGTCAGTTCCCGGA-3′, were used for constructing the template oligonucleotides as described below. A 32-mer oligonucleotide without the PhIP adduct, p32A, was used as a control template (see Table 1). Its 3′ complementary 29-, 28-, 27-, 26-, 22-, and 17-mer sequences (p29, p28, p27, p26, p22, and p17) were used as extension primers (see Table 1).

Construction of Template-Primer Complexes Containing the PhIP Adduct—A 32-mer template oligonucleotide p32C (see Table 1) was constructed by ligation of p9C with p23a as follows. The 5′-end of p23a was phosphorylated by T4 polynucleotide kinase and ATP. A mixture of p9C, p23a, and p23b (3 nmol each) in 250 μl of a buffer containing 5 mM Tris-HCl, 0.5 mM EDTA, 50 mM NaCl, pH 8.0, was denatured for 5 min at 95 °C, incubated for 10 min at 60 °C, and then cooled slowly to form the partial duplex structure of these three oligonucleotides (supplemental Fig. S1). The sample of the duplex oligonucleotide was mixed with 190 μl of Milli-Q water and 50 μl of ×10 ligation buffer (500 mM Tris-HCl (pH 7.5), 100 mM $MgCl_2$, 100 mM DTT, 10 mM ATP). Ligation was initiated by adding 10 μl of T4 DNA ligase (4,000 units), and the mixture was then incubated for 20 h at 16 °C. An additional incubation at 37 °C for 60 min was carried out after the addition of 1 μl of T4 DNA ligase, and the reaction was stopped by further incubation at 68 °C for 10 min. The p32C was separated by 18% PAGE containing 8 M urea, and excised and eluted as described previously (28). p32B and p32D were constructed using a similar method as for p9B and p9D, respectively (see Table 1). The purities of these oligonucleotides, p32B, p32C, and p32D, were determined by denatured PAGE after 5′-end labeling and UV absorbance at 260 and 370 nm.

Primer oligonucleotides were labeled with ^{32}P at the 5′-end as described previously (29), and then purified by MicroSpin™ G-25 or G-50 columns (GE Healthcare) as recommended by the supplier. The mixture of template and labeled primer (50 pmol each) in 400 μl of a buffer containing 8 mM Tris-HCl, 0.8 mM EDTA, 150 mM KCl (pH 8.0) was heated at 70 °C for 7 min, and then cooled slowly to room temperature. In the case of the substrates for TLS polymerases, pol η, pol ι, pol κ, and REV1, the final concentrations of template-primer and the constituents of the annealing buffers were changed to 500 nM and 10 mM Tris-HCl, 1 mM EDTA, and 50 mM NaCl (pH 8.0), respectively.

In Vitro DNA Synthesis Assay—A primer extension reaction was performed as described previously (30) with some modifications. Briefly, an aliquot of 0.75 μl of this primer-annealed template (final concentration, 12.5 nM) was mixed with 0.75 μl of ×10 Klenow buffer (100 mM Tris-HCl (pH 7.5), 70 mM $MgCl_2$, 1 mM DTT), 0.5 μl of 500 mM KCl, 0.5 μl of dNTP mixture (50 μM each), and 4.5 μl of Milli-Q water. After addition of 0.5 μl of Klenow fragment, the mixture was incubated at 37 °C for 10 min. The reaction was terminated by adding 1.5 μl of stop solution (160 mM EDTA, 0.7% SDS, 6 mg/ml proteinase K), and the samples were incubated at 37 °C for 30 min. Subsequently, 5.5 μl of the gel loading solution (30 mM EDTA, 0.05% bromophenol blue, 0.05% xylene cyanol, 97% formamide) was added to the samples. For pol δ, a ×10 reaction buffer containing 200 mM PIPES (pH 6.8), 20 mM $MgCl_2$, 10 mM 2-mercaptethanol, 200 μg/ml bovine serum albumin, and 50% glycerol was used instead of the buffer described above, and the reaction was carried out at 37 °C for 10 min. For other DNA polymerases, pol α, pol I, r*Taq*, and *Tth*, the constituent of each ×10 reaction buffer was altered as recommended by the suppliers.

The reaction using pol κ was performed as described above with some modifications. Briefly, an aliquot of 0.5 μl of this primer-annealed template (final 50 nM) was mixed with 0.5 μl of 10 × TLS buffer (250 mM Tris-HCl (pH 7.0), 50 mM $MgCl_2$, 50 mM DTT, 1 mg/ml bovine serum albumin), 0.5 μl of dNTP solution, and 3.0 μl of Milli-Q water. After addition of 0.5 μl of pol κ, the mixture was incubated at 30 °C for 20 min. The reac-

tion was terminated by adding 8.8 μl of the gel loading solution and a further incubation at 95 °C for 3 min. The reaction of REV1 was performed in the same manner as the reaction of pol κ with the exception that the standard reaction time was 5 min. For pol η, a ×10 reaction buffer containing 400 mM Tris-HCl (pH 8.0), 10 mM $MgCl_2$, 100 mM DTT, 1 mg/ml bovine serum albumin, and 450 mM KCl was used instead of the ×10 TLS buffer. The ^{32}P-labeled fragments were denatured and electrophoresed in a 9.5% polyacrylamide gel containing 8 M urea. The radioactivity of the fragments was determined using a Bio-Imaging Analyzer (BAS2500, Fuji Photo Film, Kanagawa, Japan). Kinetic parameters were determined by steady-state gel kinetic assays under similar conditions as described above. The incubation time for pol κ was changed to 10 min. K_m and k_{cat} were evaluated from the plot of the initial velocity *versus* the dCTP or dGTP concentration using a hyperbolic curve-fitting program in SigmaPlot 11 (Systat Software, Inc.). Data from two or three independent experiments were plotted together.

RESULTS

Construction of Template Oligonucleotides Containing a PhIP Adduct—We designed oligonucleotides containing a dG-C8-PhIP adduct at specific sites for use as templates in *in vitro* DNA synthesis analyses. For this purpose, we selected the 5′-TCCGGGAAC-3′ sequence as: 1) it corresponds to codon 868–870 of the rat *Apc* gene, one of three mutation hot spots (a single base deletion of G) in PhIP-induced colon tumors (21), and could thus be used as a model template that would reconstitute mutations of this gene; 2) two other mutation hot spots in the rat *Apc* gene and many mutated sites induced by PhIP in cultured cells and animal models contain 5′-GGGA-3′ as a core sequence (17–20). We thus speculated that the 5′-TCCGGGAAC-3′ sequence could be used as a model sequence for these GGGA to GGA mutations to some extent; and 3) some mutagenic compounds forming dG adducts, including PhIP, are expected to react preferentially with the 5′-G of a GG dinucleotide site when compared with a single G residue (31). We thus selected a sequence containing GGG as a template for our initial analysis.

We have recently synthesized three 9-mer oligonucleotides separately harboring a PhIP adduct on each G within the sequence 5′-TCC GGG AAC-3′ (22). Three 32-mer template oligonucleotides, p32B, p32C, and p32D, were constructed in our present study by ligation of these 9-mer oligonucleotides containing the dG-PhIP adduct with a 23-mer oligonucleotide, p23a, (Table 1 and supplemental Fig. S1). The purities of these oligonucleotides were tested after resolution by electrophoresis. In our present study, we principally describe the results of our *in vitro* DNA synthesis analysis using p32C as the template to avoid complexity.

In Vitro DNA Synthesis by A- and B-family DNA Polymerase—Many of the chemical compounds that can form DNA adducts *in vivo* and that show mutagenicity have been reported to impede the progress of DNA synthesis to different extents. The molecular size of PhIP is greater than most other mutagenic chemicals that form adducts. Hence, dG-PhIP was expected to block DNA synthesis to a considerable extent. To examine the effects of the dG-C8-PhIP adduct upon DNA synthesis, primer

TABLE 1
Oligonucleotide templates and primers

Oligonucleotide	Sequence[a]
p32A	5′-TCC GGG AAC TGACTCGTC GTGACTGGG AAAAC-3′
p32B	5′-TCC GGG AAC TGACTCGTC GTGACTGGG AAAAC-3′
p32C	5′-TCC GGG AAC TGACTCGTC GTGACTGGG AAAAC-3′
p32D	5′-TCC GGG AAC TGACTCGTC GTGACTGGG AAAAC-3′
p29	5′-GTT TTC CCA GTCACGACG AGTCAGTTC CC-3′
p28	5′-GTT TTC CCA GTCACGACG AGTCAGTTC C-3′
p27	5′-GTT TTC CCA GTCACGACG AGTCAGTTC-3′
p26	5′-GTT TTC CCA GTCACGACG AGTCAGTT-3′
p22	5′-GTT TTC CCA GTCACGACG AGTC-3′
p17	5′-GTT TTC CCA GTCACGAC-3′

[a] The bold G indicates the site of the PhIP-C8-dG adduct. Underlined sequences correspond to codon 868–870 at nucleotides 2602–2610 of the rat APC gene.

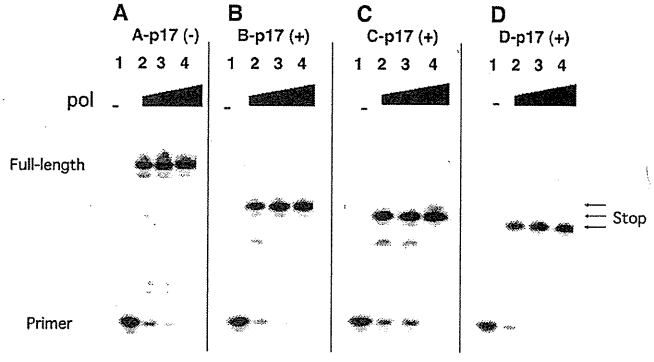

FIGURE 2. ***In vitro* DNA synthesis using Klenow fragment.** Gel electrophoresis indicating the primer extensions obtained using the 32-mer oligonucleotide templates, p32A (*A*), p32B (*B*), p32C (*C*), and p32D (*D*), which have no PhIP adduct, and a PhIP adduct on the first, second, and third G within the triple G sequence, respectively. The 3′ complementary 17-mer sequence, p17, was used as the extension primer. The final concentration of each template-primer complex was 12.5 nM. Concentrations of Klenow fragment were 0 (*lane 1*), 7.8 (*lane 2*), 23 (*lane 3*), and 78 units/ml (*lane 4*).

extension experiments using p32B, p32C, and p32D as templates were carried out (see Table 1). The length of each produced fragment was precisely determined using ladders of oligonucleotide fragments as markers (data not shown). The Klenow fragment of *E. coli* DNA polymerase I, a member of the A-family DNA polymerases, was first used in this analysis. The production of a 28-, 27-, and 26-mer from these primer extension reactions using B-p17, C-p17, and D-p17, respectively, using a template-primer complex, and lack of longer fragments indicated that the Klenow fragment stalled just before the dG-C8-PhIP adduct (Fig. 2). On the other hand, control experiments using p32A without the adduct as a template produced a 32-mer fragment (Fig. 2*A*). Similar results were obtained with *E. coli* DNA polymerase I (exo$^+$) and B-family DNA polymerases, such as the thermophilic bacterial DNA polymerases, r*Taq* and *Tth*, and human DNA polymerase α (data not shown) (supplemental Fig. S2), suggesting that stalling at the dG-C8-PhIP adduct occurs for all replicative DNA polymerases. Stalling of r*Taq* and *Tth* at the PhIP adduct was observed at 65 °C, as well as at 37 °C, indicating that this is the result of a physical hindrance of the adduct itself and not from secondary DNA structures. Moreover, there was no difference found between the stalling of *E. coli* DNA polymerase I (exo$^+$) and that of the Klenow fragment (exo$^-$). This indicates that the physical blocking of DNA polymerases at the dG-C8-PhIP adduct does not depend upon their proofreading function.

Finally, DNA synthesis analyses with human DNA polymerase δ (pol δ), a member of the B-family DNA polymerases and a truly replicative polymerase, were carried out. In the case of using p32C and p17 (C-p17) as a template-primer complex, the production of 27-mer fragments indicated the stalling of pol δ just before the PhIP adduct (Fig. 3, *lane 11*). From a control reaction using A-p17, a template-primer complex without the PhIP adduct, a full-length product of 32-mer was generated (Fig. 3, *lane 8*). In addition to these major products, minor products extended one nucleotide further (28- and 33-mer) and ladders of bands indicating degradation of primer (<17-mer) were observed (Fig. 3), corresponding with previous results reporting terminal dA transferase and exonuclease activities of pol δ (32). PCNA, an accessory protein acting as a sliding clamp for pol δ, was previously reported to promote DNA synthesis by pol δ past several template lesions, including abasic sites, 8-oxo-dG, and aminofluorene-dG (32). In the case of dG-C8-PhIP, however, PCNA was unable to promote the bypass synthesis of pol δ beyond the lesion (Fig. 3, *lane 12*). Extension reaction from the longer 22-mer primer, p22, also paused completely just before the PhIP adduct in the presence or absence of PCNA (Fig. 3, *lanes 5* and *6*). These results strongly suggest that the dG-C8-PhIP adduct on genome DNA in the living cells induces the complete block of replication forks including pol δ, PCNA, and pol α.

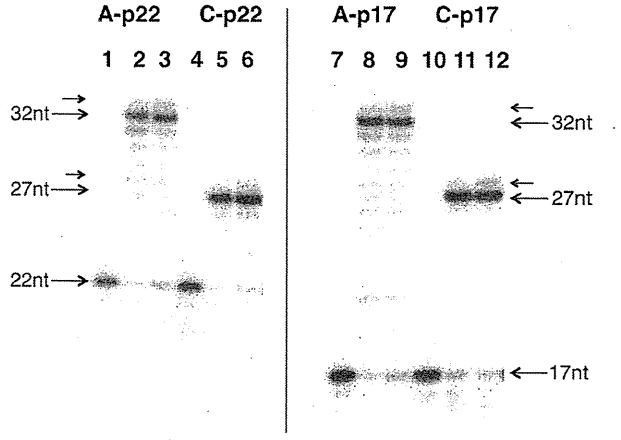

FIGURE 3. ***In vitro* DNA synthesis using pol δ in the presence or absence of PCNA.** Gel electrophoresis indicating the primer extensions obtained using the 32-mer oligonucleotide templates, p32A (*A*), and p32C (*C*), which have no PhIP adduct, and a PhIP adduct on the second G within the triple G sequence, respectively. The 3′ complementary 22- and 17-mer sequences, p22 and p17, were used as the extension primer. The final concentration of each template-primer complex was 12.5 nM. Concentrations of pol δ were 0 (*lanes 1, 4, 7,* and *10*) and 16 nM (*lanes 2, 3, 5, 6, 8, 9, 11,* and *12*). Concentrations of PCNA as a trimer were 0 (*lanes 1, 2, 4, 5, 7, 8, 10,* and *11*) and 20 nM (*lanes 3, 6, 9,* and *12*). *Large arrows* indicate the positions of primers (17- or 22-mer), full-length products (32-mer), and the products pausing just before the PhIP adduct (27-mer). *Small arrows* indicate the minor products that incorporated an additional 1 nucleotide (*nt*) to a full-length product or the pausing product.

Translesional DNA Synthesis by Y-family DNA Polymerases—Translesional DNA synthesis at the dG-C8-PhIP adduct by the Y-family DNA polymerases, pol η, pol κ, pol ι, and REV1 was next examined. Two substrates, C-p27 and C-p28, and their counterparts without a PhIP adduct, A-p27 and A-p28, were used in these experiments (Fig. 4). Substrate C-p27 was prepared by annealing the p32C template (see Table 1) to its 3′-complimentary 27-mer sequence, p27, and was used to identify the nucleotides that are inserted opposite the dG-C8-PhIP adduct (Fig. 4). Similarly, substrate C-p28 was used to analyze the extension reaction from the 3′-end of the dC bases opposite the dG-C8-PhIP adduct (Fig. 4). We found that recombinant human DNA polymerase η (pol η) could insert a dC opposite the dG-C8-PhIP adduct, although at low efficiency compared with control experiments without the PhIP adduct (Fig. 5, *A* and *B*). Extension reactions catalyzed by pol η from the 3′-end of dC opposite the adduct were barely detectable (Fig. 5*D*), although an excessive amount of pol η produced byproducts that incorporated a mismatch nucleotide, dG, dA, or dT (supplemental Fig. S4). In the case of dG, incorporation of one to three dG nucleotides was observed (supplemental Fig. S4). In control experiments without the PhIP adduct, minor products were produced that incorporated mismatch nucleotides, in addition to a major product that incorporated a dC (Fig. 5*C*).

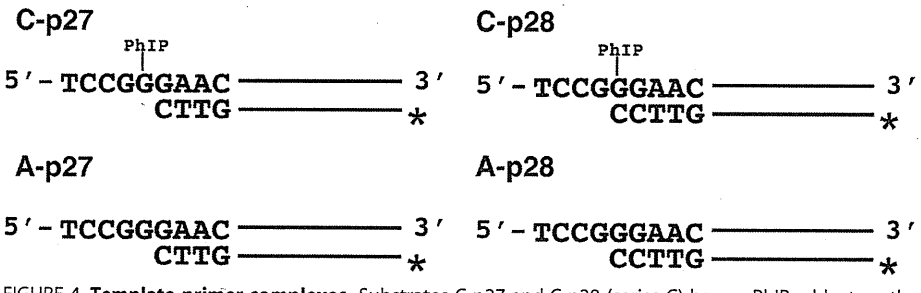

FIGURE 4. **Template-primer complexes.** Substrates C-p27 and C-p28 (series-C) have a PhIP adduct on the second dG within a GGG sequence. Substrates A-p27 and A-p28 (series-A) are control substrates without a PhIP adduct. The corresponding 3′ complimentary 27- and 28-mer sequences, p27 and p28, were used as extension primers. The template-primer complexes, C-p27 and C-p28, were used to monitor the nucleotide insertions into the site opposite dG-C8-PhIP and the extension reactions from the 3′-dC opposite dG-C8-PhIP, respectively.

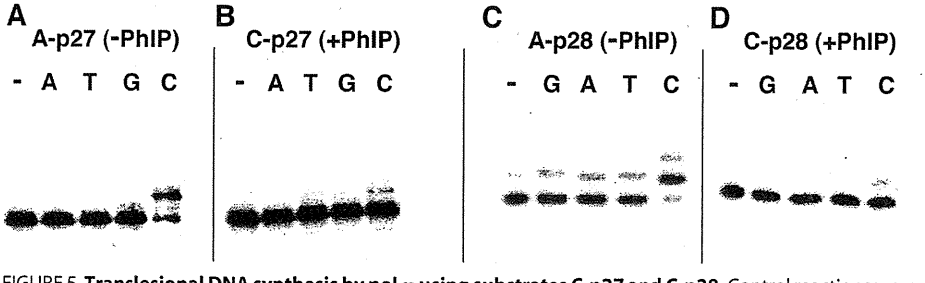

FIGURE 5. **Translesional DNA synthesis by pol η using substrates C-p27 and C-p28.** Control reactions were performed using substrates without the PhIP adduct, A-p27 (*A*) and A-p28 (*C*). An insertion reaction was performed with substrate C-p27 (*B*) and an extension reaction with substrate C-p28 (*D*). A single dNTP (G, A, T, C) was added into the reaction mixture as indicated by *G, A, T,* and *C above* each lane. The lanes indicated by — are controls without any nucleotides. Concentrations of pol η and each dNTP were 1.9 nM and 100 μM, respectively.

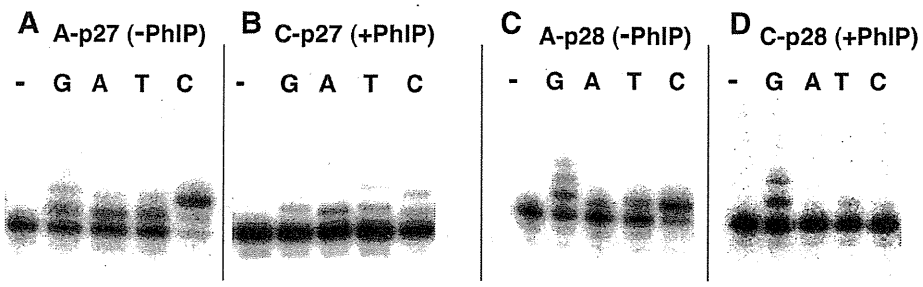

FIGURE 6. **Translesional DNA synthesis by pol κ using substrates C-p27 and C-p28.** Control reactions were performed using substrates without the PhIP adduct, A-p27 (*A*) and A-p28 (*C*). An insertion reaction was performed with substrate C-p27 (*B*) and an extension reaction with substrate C-p28 (*D*). A single dNTP (G, A, T, C) was added into the reaction mixture as indicated by *G, A, T,* and *C above* each lane. The lanes indicated by − are controls without any nucleotides. The concentrations of pol κ were 250 (*A* and *C*), 500 (*B*), and 1000 nM (*D*), respectively. The concentration of each dNTP was 100 μM.

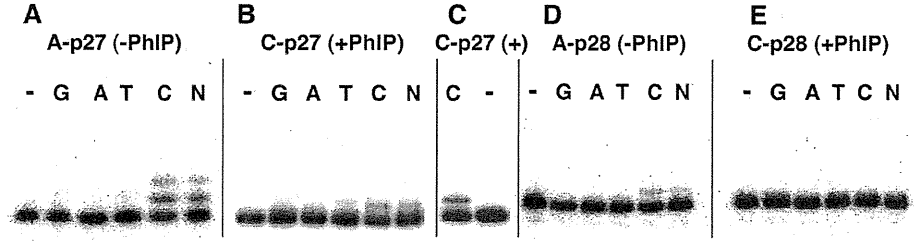

FIGURE 7. **Translesional DNA synthesis by REV1 using substrates C-p27 and C-p28.** Control reactions were performed using substrates without the PhIP adduct, A-p27 (*A*) and A-p28 (*D*). Insertion reactions were performed with substrate C-p27 (*B* and *C*) and an extension reaction with substrate C-p28 (*E*). A single dNTP (G, A, T, and C) or a mixture of each was added into the reaction mixture as indicated by *G, A, T, C,* and *N above* each lane. The lanes indicated by − are controls without any nucleotides. The concentrations of REV1 were 5.2 (*A* and *D*) and 26 nM (*B, C,* and *E*), respectively. The concentrations of each dNTP were 100 μM (*A, B, D,* and *E*) and 320 μM (*C*), respectively. The *N* mixture contained each dNTP at a concentration of 25 μM.

We next examined translesional DNA synthesis beyond the PhIP adduct using a truncated form of human DNA polymerase κ containing the N-terminal 559 amino acids. One or two dCs were inserted opposite the dG-C8-PhIP adduct by this polymerase, and misinsertions of three other nucleotides were also observed to a certain extent (Fig. 6*B*). pol κ incorporated two dCs and misincorporated dG, dA, and dT into the A-p27 substrate without the PhIP adduct at a low efficiency (Fig. 6*A*). Misincorporations of dG, dA, and dT into the A-p28 substrate without the adduct were also observed (Fig. 6*C*). In the case of the extension reaction from 3′-dC opposite the dG-PhIP adduct, pol κ also incorporated dC and misincorporated dT into the C-p28 substrate at low efficiency (Fig. 6*D*). Interestingly, one- and two-base incorporations of dG into the substrate C-p28 by pol κ dominated the incorporation of a dC (Fig. 6*D*). In the extension reaction with pol κ in the presence of all four dNTPs, fragments of 29 and 30 nucleotides were observed as major products, and a small amount of the 31-nucleotide fragment was observed (see supplemental Fig. S5, *lane 6*). Full-length products of 32 nucleotides were observed only when an excess amount of pol κ was present (data not shown). This poor extension activity of pol κ after adding two nucleotides was probably caused by the shortness (~4 nucleotides) of the 5′ region to the lesion in the template oligonucleotide. Extension with pol κ, pol η, and pol δ from the mismatched primers, where the 3′-terminal nucleotide of the p28 primer, dC, was substituted with another nucleotide, could not be observed (data not shown). REV1 inserted a dC opposite the PhIP adduct at a higher efficiency compared with pol κ and pol η (Fig. 7, *B* and *C*). REV1 was, however, unable to catalyze the extension reaction from the dC opposite the PhIP adduct in C-p28 (Fig. 7*E* and supplemental Fig. S5, *lane 5*). REV1 incorporated only dC nucleotides into A-p27 and A-p28 substrates without the adduct (Fig. 7, *A* and *D*). Neither nucleotide insertion nor extension reactions for the templates containing the PhIP adduct were detected using human pol ι (data not shown).

Kinetic Analyses of Translesional DNA Synthesis by pol κ and REV1—To evaluate translesional DNA synthesis beyond the dG-C8-PhIP adduct in further detail, additional quantitative analyses for pol κ and REV1 were performed. Insertion reactions catalyzed by pol κ for dC (Fig. 8, *B, lanes 2–5,* and *C, closed diamonds*) and dG (Fig. 8, *B, lanes 6–9,* and *C, closed triangles*) into substrate C-p28 were analyzed in the same way. Kinetic parameters for pol κ were determined using steady-state kinetic assays (Table 2). The catalytic efficiency (k_{cat}/K_m) of dC insertion into C-p28 (0.039 min^{-1} mM^{-1}) was found to be 4-fold greater than that into C-p27 (0.011 min^{-1} mM^{-1}). These results indicate that pol κ catalyzes the extension reaction from the 3′-terminal of dC opposite the dG-C8-PhIP with a higher efficiency than the insertion reaction opposite the adduct. The k_{cat}/K_m values of the dC insertion opposite the adduct were roughly 4 orders of magnitude less than those into counterparts without the adduct (see Table 2). The k_{cat}/K_m value of the dG incorporation into C-p28 was slightly higher than that of dC, and more than 8-fold higher than that of dG into C-p27 (see Table 2). This result indicates that pol κ skipped over the dG site just 5′ of dG-C8-PhIP on the template and incorporated dG opposite dC on the template strand of substrate C-p28 with a high efficiency. The k_{cat}/K_m values of the dC incorporation into D-p27 (0.19 min^{-1} mM^{-1}) were over 4-fold greater than into C-p28 (0.039 min^{-1} mM^{-1}) and over 8-fold higher than that of dG into B-p29 (0.023) (see supplemental Table S1). These data indicate that the efficiencies of the extension reaction by pol κ are the highest for template p32D containing the PhIP adduct in the third G of the triple G run, next for template p32C containing the PhIP/adduct in the second G, and lowest for template p32B containing the PhIP adduct in the first G.

Even at higher concentrations of dNTPs, extension reactions catalyzed by REV1 for substrate C-p28 could not be monitored (Table 3, Fig. 7*E*). The k_{cat}/K_m value of the dC incorporation by REV1 into substrate C-p27 was more than 2,000 times greater than that by pol k, and 1/44 of the values for counterparts with-

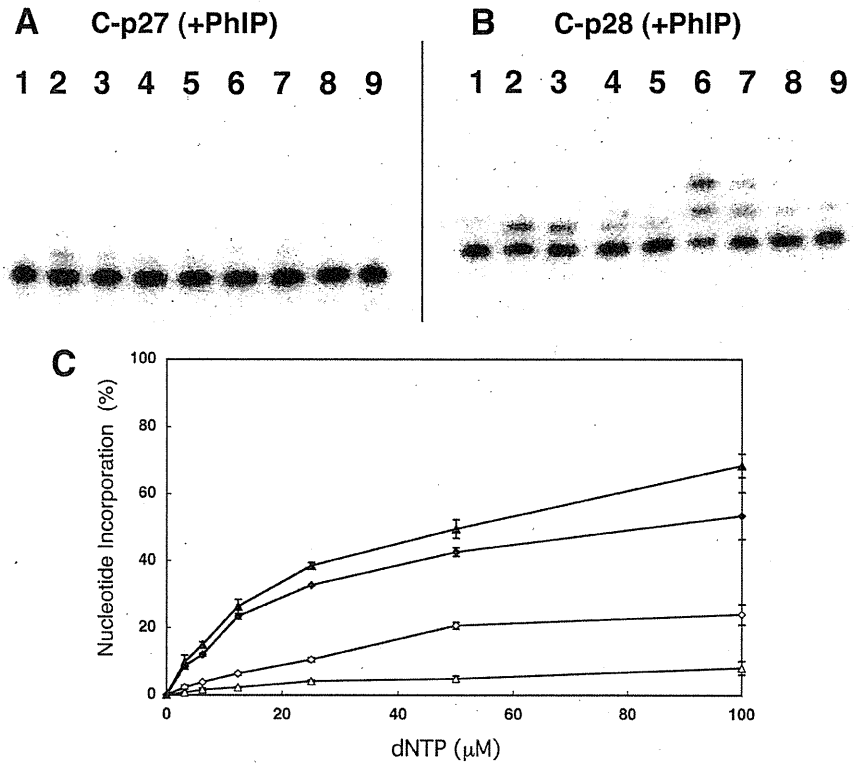

FIGURE 8. **Translesional DNA synthesis by pol κ.** Nucleotide incorporation by pol κ for substrates C-p27 (*A*) and C-p28 (*B*). Either dCTP (*lanes 2-5*) or dGTP (*lanes 6-9*) was added into the reaction mixture. *Lane 1* indicates a control without any nucleotides. The concentration of pol κ was 910 nM. The concentrations of dCTP or dGTP, respectively, were 25 (*lanes 2* and *6*), 12.5 (*lanes 3* and *7*), 6.25 (*lanes 4* and *8*), and 3.13 μM (*lanes 5* and *9*). *C*, incorporation efficiencies of dCTP and dGTP into substrate C-p27 and C-p28. Incorporations of dCTP into C-p27, dGTP into C-p27, dCTP into C-p28, and dGTP into C-p28 are indicated by *open diamonds*, *open triangles*, *closed diamonds*, and *closed triangles*, respectively. Each data point represents the mean of two separate experiments. The *error bars* represent residuals.

TABLE 2
k_{cat}/K_m values for pol κ

Substrate	K_m	k_{cat}	k_{cat}/K_m
	μM	$\times 10^{-3}$ min^{-1}	min^{-1} mM^{-1}
C-p27			
dCTP	70	0.76	0.011
dGTP	47	0.24	0.0050
C-p28			
dCTP	8.0	0.32	0.039
dGTP	11	0.48	0.042
A-p27			
dCTP	0.035	4.4	130
dGTP	0.26	1.3	5.0
A-p28			
dCTP	0.027	3.7	140
dGTP	2.1	8.8	4.1

TABLE 3
k_{cat}/K_m values for dCTP-insertion by REV1

Substrate	K_m	k_{cat}	k_{cat}/K_m
	μM	$\times 10^{-3}$ min^{-1}	min^{-1} mM^{-1}
C-p27	12	320	27
C-p28	ND[a]	ND	ND
A-p27	0.36	390	1100

[a] ND, not detectable.

out the adduct (Table 3). The k_{cat}/K_m values of the dC insertion by REV1 into three substrates, B-p28, C-p27 and D-p26, were 39, 27, and 73 min^{-1} mM^{-1}, respectively. Thus, the insertion reaction catalyzed by REV1 among the three templates was the most efficient for template p32D containing the PhIP adduct at the third G, similar to the extension reaction by pol κ.

DISCUSSION

In Vitro TLS Analysis Reconstituting PhIP-induced Mutations—HCAs are food-borne carcinogens produced when cooking meat (1, 9, 33). The most significant aspect of these molecules is that they exist normally in cooked food and are thus ubiquitous carcinogens (32). The mutagenicity and carcinogenicity of HCAs are mainly attributed to C8- and N2-dG adducts (9). Both excision repair and translesional DNA synthesis play critical roles in the mutagenesis steps induced by HCAs. However, despite the importance of HCAs as common environmental mutagens, there have been very few previous reports regarding the stalling of DNA polymerases and TLS caused by the DNA adducts they form. This is mainly because of the difficulty in preparing template DNA with introduced HCA adducts at specific sites. Choi *et al.* (34) have recently undertaken a biochemical study of TLS at adducts of the HCA 2-amino-3-methylimidazo[4,5-*f*]quinoline (IQ) using purified human polymerases. In our current study of TLS, we describe our findings for adducts of PhIP, the most abundant HCA in cooked foods (4).

A rat colon cancer model induced by PhIP shows profiles of cancer development similar to the multistep model of colon carcinogenesis in humans (35). In this rat model, *p53* and K-*ras* mutations are rarely observed, whereas mutations in *Apc* and its downstream gene *β-catenin* have been frequently observed (21, 36–38). Hence, mutations in *Apc* or *β-catenin* have been speculated to play a critical role in PhIP-induced colon carcinogenesis. Five mutations in the *Apc* gene were previously detected in four of eight PhIP-induced rat colon tumors, and all of these mutations involved a single guanine deletion in the 5′-GGGA-3′ sequence (21). This characteristic mutation induced by PhIP, 5′-GGGA-3′ to 5′-GGA-3′, was also observed in other *in vivo* mutation analyses using transgenic animals harboring introduced reporter genes, such as *lacI* (18–20). Hence, the 5′-TCCGGGAAC-3′ sequence corresponding to a mutation hot spot within the rat *Apc* gene, which we utilized to introduce the PhIP adduct and employed as the template for *in vitro* DNA synthesis analyses, could be a suitable model for revealing the molecular mechanisms associated with PhIP-induced mutations.

As discussed later, our results indicate a possible molecular mechanism for the 5′-GGGA-3′ to 5′-GGA-3′ mutation induced by PhIP.

DNA Polymerases Involved in TLS through the dG-PhIP Adduct—TLS through many DNA lesions requires the action of two different polymerases, an "inserter" and an "extender," the former to perform nucleotide insertions opposite the lesion site and the latter for subsequent extensions (39). The catalytic efficiency of the dCTP-insertion reaction opposite the dG-PhIP adduct by REV1 was found to be more than 2,000-fold greater than that by pol κ (see Tables 2 and 3). This result strongly suggests that REV1 functions *in vivo* as an inserter polymerase for TLS through the dG-PhIP adduct. This insertion step by REV1 is also error free. REV1 has been reported previously to insert dCTP opposite abasic sites and various N2-dG adducts (26, 39–41). However, our current study is the first to show that REV1 inserts dCTP opposite a large size C8-dG adduct. We used a shorter (C-terminal deleted) form of pol κ in our current experiments and an intact pol κ may be more effective for this insertion reaction. As for pol η, a detailed kinetic analysis was not performed. Hence, the possibility cannot be excluded that pol κ and pol η also function as inserter polymerases.

In addition to the Y-family DNA polymerases, DNA polymerase ζ (pol ζ), belonging to the B-family DNA polymerases, is considered to be involved in TLS through various lesions as an extender DNA polymerase (39, 42, 43). We have not carried out a primer extension assay with pol ζ and thus the possibility cannot be completely excluded by our current data that pol ζ functions *in vivo* as an extender polymerase for TLS through the dG-PhIP adduct. In our present study, we provide evidence that pol κ can extend from dC opposite the dG-C8-PhIP adduct *in vitro*. It is, therefore, possible that pol κ, at least partially, functions as an extender polymerase *in vivo* for TLS through the dG-PhIP adduct. Further study about cooperation between two or more DNA polymerases, including pol ζ, is necessary to verify which DNA polymerases are involved in the bypass synthesis through the PhIP lesion.

The catalytic efficiency of pol κ for a dGTP insertion into substrate C-p28 was a little higher than that for dCTP insertions (see Table 2 and Fig. 6*D*). The former generates a single guanine deletion, and the latter is an error-free extension. Consequently, our data suggest that the extension reaction with pol κ from the nucleotide opposite the dG-C8-PhIP adduct causes frequent single-guanine deletions from the GGG stretch. It has been reported that one characteristic feature of pol κ homologs, from bacteria to humans, is their propensity to generate single-base deletions (44–47). The crystal structure of Dpo4, a thermophilic archaea homolog of pol κ, in ternary complexes with DNA and an incoming nucleotide supports the model that a single base deletion by pol κ is generated through a misaligned intermediate complex where the template dG forms an extrahelical looped out structure and the incoming dGTP skips this extrahelical base and pairs with the next template base dC (48) (see supplemental Fig. S6). It is reasonable to speculate therefore that, in the case of TLS through dG-C8-PhIP, mammalian pol κ generates the single guanine deletion via a similar intermediate where the PhIP-adducted dG is looped out and template-primer slippage occurs. However, further analyses for determining whether the one-base skipping of pol κ beyond the lesion observed by us is dependent on the nucleotide placed 5′ to the lesion or not, are necessary to clarify the detailed molecular mechanism underlying one base skipping of pol κ.

Molecular Mechanisms Underlying Mutation Induction by PhIP—We have demonstrated herein by *in vitro* DNA synthesis analyses using oligonucleotide templates containing dG-PhIP that: 1) replicative DNA polymerases stall at the PhIP adduct and cannot perform translesional DNA synthesis beyond this point; 2) REV1 inserts a dC opposite the dG-PhIP with a much higher efficiency than other TLS polymerases, including pol κ and pol η; and 3) pol κ has a potential ability to catalyze an extension reaction from the 5′-dC opposite the adduct and often skips over one dG in the template during this extension step. A working model for the induction of mutations at the PhIP adducts based on the results shown in the present study is illustrated in supplemental Fig. S6. This model could be adopted for other sequences containing a G repeat stretch longer than GGG.

REFERENCES

1. Nagao, M. (2000) in *Food Borne Carcinogens: Heterocyclic Amines* (Nagao, M., and Sugimura, T., eds) pp. 163–196, John Wiley & Sons Ltd., Chichester, UK
2. Schut, H. A., and Snyderwine, E. G. (1999) *Carcinogenesis* **20,** 353–368
3. Felton, J. S., Knize, M. G., Shen, N. H., Lewis, P. R., Andresen, B. D., Happe, J., and Hatch, F. T. (1986) *Carcinogenesis* **7,** 1081–1086
4. Felton, J. S., Jagerstad, M., Knize, M. G., Skog, K., and Wakabayashi, K. (2000) in *Food Borne Carcinogens: Heterocyclic Amines* (Nagao, M., and Sugimura, T., eds) pp. 31–71, John Wiley & Sons Ltd., Chichester, UK
5. Holme, J. A., Wallin, H., Brunborg, G., Søderlund, E. J., Hongslo, J. K., and Alexander, J. (1989) *Carcinogenesis* **10,** 1389–1396
6. Felton, J. S., and Knize, M. G. (1991) *Mutat. Res.* **259,** 205–217
7. Ohgaki, H., Takayama, S., and Sugimura, T. (1991) *Mutat. Res.* **259,** 399–410
8. Ito, N., Hasegawa, R., Sano, M., Tamano, S., Esumi, H., Takayama, S., and Sugimura, T. (1991) *Carcinogenesis* **12,** 1503–1506
9. Sugimura, T., Wakabayashi, K., Nakagama, H., and Nagao, M. (2004) *Cancer Sci.* **95,** 290–299
10. Imaida, K., Hagiwara, A., Yada, H., Masui, T., Hasegawa, R., Hirose, M., Sugimura, T., Ito, N., and Shirai, T. (1996) *Jpn. J. Cancer Res.* **87,** 1116–1120
11. Frandsen, H., Grivas, S., Andersson, R., Dragsted, L., and Larsen, J. C. (1992) *Carcinogenesis* **13,** 629–635
12. Lin, D., Kaderlik, K. R., Turesky, R. J., Miller, D. W., Lay, J. O., Jr., and Kadlubar, F. F. (1992) *Chem. Res. Toxicol.* **5,** 691–697
13. Snyderwine, E. G., Davis, C. D., Nouso, K., Roller, P. P., and Schut, H. A. (1993) *Carcinogenesis* **14,** 1389–1395
14. Schut, H. A., and Herzog, C. R. (1992) *Cancer Lett.* **67,** 117–124
15. Endo, H., Schut, H. A., and Snyderwine, E. G. (1994) *Cancer Res.* **54,** 3745–3751
16. Morgenthaler, P. M., and Holzhäuser, D. (1995) *Carcinogenesis* **16,** 713–718
17. Yadollahi-Farsani, M., Gooderham, N. J., Davies, D. S., and Boobis, A. R. (1996) *Carcinogenesis* **17,** 617–624
18. Okonogi, H., Stuart, G. R., Okochi, E., Ushijima, T., Sugimura, T., Glickman, B. W., and Nagao, M. (1997) *Mutat. Res.* **395,** 93–99
19. Lynch, A. M., Gooderham, N. J., Davies, D. S., and Boobis, A. R. (1998) *Mutagenesis* **13,** 601–605
20. Okochi, E., Watanabe, N., Shimada, Y., Takahashi, S., Wakazono, K., Shirai, T., Sugimura, T., Nagao, M., and Ushijima, T. (1999) *Carcinogenesis* **20,** 1933–1988
21. Kakiuchi, H., Watanabe, M., Ushijima, T., Toyota, M., Imai, K., Weisburger, J. H., Sugimura, T., and Nagao, M. (1995) *Proc. Natl. Acad. Sci.*

U.S.A. **92,** 910–914
22. Takamura-Enya, T., Ishikawa, S., Mochizuki, M., and Wakabayashi, K. (2006) *Chem. Res. Toxicol.* **19,** 770–778
23. Masuda, Y., Suzuki, M., Piao J., Gu, Y., Tsurimoto, T., and Kamiya, K. (2007) *Nucleic Acids Res.* **35,** 6904–6916
24. Masutani, C., Kusumoto, R., Iwai, S., and Hanaoka, F. (2000) *EMBO J.* **19,** 3100–3109
25. Niimi, N., Sassa, A., Katafuchi, A., Grúz, P., Fujimoto, H., Bonala, R. R., Johnson, F., Ohta, T., and Nohmi, T. (2009) *Biochemistry* **48,** 4239–10234246
26. Masuda, Y., and Kamiya, K. (2002) *FEBS Lett.* **520,** 88–92
27. Masuda, Y., Ohmae, M., Masuda, K., and Kamiya, K. (2003) *J. Biol. Chem.* **278,** 12356–12360
28. Sambrook, J., Fritsch, E. F., and Maniatis, T. (1989) *Molecular Cloning: A Laboratory Manual,* 2nd Ed., Cold Spring Harbor Laboratory, Cold Spring Harbor, NY
29. Fukuda, H., and Ohtsubo, E. (1997) *Genes Cells* **2,** 735–751
30. Fukuda, H., Katahira, M., Tsuchiya, N., Enokizono, Y., Sugimura, T., Nagao, M., and Nakagama, H. (2002) *Proc. Natl. Acad. Sci. U.S.A.* **99,** 12685–12690
31. Sugiyama, H., and Saito, I. (1996) *J. Am. Chem. Soc.* **118,** 7063–7068
32. Mozzherin, D. J., Shibutani, S., Tan, C. K., Downey, K. M., and Fisher, P. A. (1997) *Proc. Natl. Acad. Sci. U.S.A.* **94,** 6126–6231
33. Sugimura, T., and Adamson, R. H. (2000) in *Food Borne Carcinogens: Heterocyclic Amines* (Nagao, M., and Sugimura, T., eds) pp. 1–4, John Wiley & Sons Ltd., Chichester, UK
34. Choi, J. Y., Stover, J. S., Angel, K. C., Chowdhury, G., Rizzo, C. J., and Guengerich, F. P. (2006) *J. Biol. Chem.* **281,** 25297–25306
35. Nakagama, H., Ochiai, M., Ubagai, T., Tajima, R., Fujiwara, K., Sugimura, T., and Nagao, M. (2002) *Mutat. Res.* **506–507,** 137–144
36. Nagao, M. (1999) *Mutat. Res.* **431,** 3–12
37. Nagao, M., Ushijima, T., Toyota, M., Inoue, R., and Sugimura, T. (1997) *Mutat. Res.* **376,** 161–167
38. Dashwood, R. H., Suzui, M., Nakagama, H., Sugimura, T., and Nagao, M. (1998) *Cancer Res.* **58,** 1127–1129
39. Prakash, S., Johnson, R. E., and Prakash, L. (2005) *Annu. Rev. Biochem.* **74,** 317–353
40. Nelson, J. R., Lawrence, C. W., and Hinkle, D. C. (1996) *Nature* **382,** 729–731
41. Haracska, L., Prakash, S., and Prakash, L. (2002) *J. Biol. Chem.* **277,** 15546–15551
42. Johnson, R. E., Washington, M. T., Haracska, L., Prakash, S., and Prakash, L. (2000) *Nature* **406,** 1015–1019
43. Haracska, L., Unk, I., Johnson, R. E., Johansson, E., Burgers, P. M., Prakash, S., and Prakash, L. (2001) *Genes Dev.* **15,** 945–954
44. Kim, S. R., Maenhaut-Michel, G., Yamada, M., Yamamoto, Y., Matsui, K., Sofuni, T., Nohmi, T., and Ohmori, H. (1997) *Proc. Natl. Acad. Sci. U.S.A.* **94,** 13792–13797
45. Kobayashi, S., Valentine, M. R., Pham, P., O'Donnell, M., and Goodman, M. F. (2002) *J. Biol. Chem.* **277,** 34198–34207
46. Ogi, T., Kato, T., Jr., Kato, T., and Ohmori, H. (1999) *Genes Cells* **4,** 607–618
47. Ohashi, E., Bebenek, K., Matsuda, T., Feaver, W. J., Gerlach, V. L., Friedberg, E. C., Ohmori, H., and Kunkel, T. A. (2000) *J. Biol. Chem.* **275,** 39678–39684
48. Ling, H., Boudsocq, F., Woodgate, R., and Yang, W. (2001) *Cell* **107,** 91–102

Particle and Fibre Toxicology

BioMed Central

Research

Open Access

Genotoxicity of nano/microparticles in *in vitro* micronuclei, *in vivo* comet and mutation assay systems

Yukari Totsuka*[1], Takashi Higuchi[1], Toshio Imai[2], Akiyoshi Nishikawa[3], Takehiko Nohmi[4], Tatsuya Kato[5], Shuich Masuda[5], Naohide Kinae[5], Kyoko Hiyoshi[6], Sayaka Ogo[7], Masanobu Kawanishi[7], Takashi Yagi[7], Takamichi Ichinose[8], Nobutaka Fukumori[9], Masatoshi Watanabe[10], Takashi Sugimura[1] and Keiji Wakabayashi[1]

Address: [1]Cancer Prevention Basic Research Project, National Cancer Center Research Institute, 1-1 Tsukiji 5-chome, Chuo-ku, Tokyo 104-0045, Japan, [2]Central Animal Laboratory, National Cancer Center Research Institute, 1-1 Tsukiji 5-chome, Chuo-ku, Tokyo 104-0045, Japan, [3]Division of Pathology, National Institute of Health Sciences, 1-18-1 Kamiyoga, Setagaya-ku, Tokyo 158-8501, Japan, [4]Division of Genetics and Mutagenesis, National Institute of Health Sciences, 1-18-1 Kamiyoga, Setagaya-ku, Tokyo 158-8501, Japan, [5]Department of Food and Nutritional Sciences, Graduate School of Nutritional and Environmental Sciences, University of Shizuoka, 52-1, Yada, Shizuoka, 422-8526, Japan, [6]Fundamental Nursing, School of Nursing, University of Shizuoka, 52-1, Yada, Shizuoka, 422-8526, Japan, [7]Environmental Genetics Laboratory, Frontier Science Innovation Center, Osaka Prefecture University, 1-2 Gakuen-cho Naka-ku, Sakai-city, Osaka, 599-8570, Japan, [8]Department of Health Sciences, Oita University of Nursing and Health Sciences, 2944-9 Megusuno, Oita-city, Oita, Japan, [9]Department of Environmental Health and Toxicology, Tokyo Metropolitan Institute of Public Health, 24-1, Hyakunin-cho 3-Chome, Shinjuku-ku, Tokyo, 169-0073, Japan and [10]Division of Materials Science and Engineering, Yokohama National University, Graduate School of Engineering, 79-5, Tokiwadai, Hodogaya-ku, Yokohama, 240-8501, Japan

Email: Yukari Totsuka* - ytotsuka@gan2.res.ncc.go.jp; Takashi Higuchi - tahiguch@ncc.go.jp; Toshio Imai - toimai@ncc.go.jp; Akiyoshi Nishikawa - nishikaw@nihs.go.jp; Takehiko Nohmi - nohmi@nihs.go.jp; Tatsuya Kato - p7107@mail.u-shizuoka-ken.ac.jp; Shuich Masuda - masudas@u-shizuoka-ken.ac.jp; Naohide Kinae - kinae@u-shizuoka-ken.ac.jp; Kyoko Hiyoshi - hiyoshi@u-shizuoka-ken.ac.jp; Sayaka Ogo - es04509@riast.osakafu-u.ac.jp; Masanobu Kawanishi - kawanisi@riast.osakafu-u.ac.jp; Takashi Yagi - yagi-t@riast.osakafu-u.ac.jp; Takamichi Ichinose - ichinose@oita-nhs.ac.jp; Nobutaka Fukumori - Nobutaka_Fukumori@member.metro.tokyo.jp; Masatoshi Watanabe - mawata@ynu.ac.jp; Takashi Sugimura - tsugimur@ncc.go.jp; Keiji Wakabayashi - kwakabay@ncc.go.jp

* Corresponding author

Published: 3 September 2009

Particle and Fibre Toxicology 2009, **6**:23 doi:10.1186/1743-8977-6-23

Received: 1 May 2009
Accepted: 3 September 2009

This article is available from: http://www.particleandfibretoxicology.com/content/6/1/23

Abstract

Background: Recently, manufactured nano/microparticles such as fullerenes (C_{60}), carbon black (CB) and ceramic fiber are being widely used because of their desirable properties in industrial, medical and cosmetic fields. However, there are few data on these particles in mammalian mutagenesis and carcinogenesis. To examine genotoxic effects by C_{60}, CB and kaolin, an *in vitro* micronuclei (MN) test was conducted with human lung cancer cell line, A549 cells. In addition, DNA damage and mutations were analyzed by *in vivo* assay systems using male C57BL/6J or *gpt* delta transgenic mice which were intratracheally instilled with single or multiple doses of 0.2 mg per animal of particles.

Results: In *in vitro* genotoxic analysis, increased MN frequencies were observed in A549 cells treated with C_{60}, CB and kaolin in a dose-dependent manner. These three nano/microparticles also induced DNA damage in the lungs of C57BL/6J mice measured by comet assay. Moreover, single or multiple instillations of C_{60} and kaolin, increased either or both of *gpt* and Spi- mutant frequencies in the lungs of *gpt* delta transgenic mice. Mutation spectra analysis showed transversions were

predominant, and more than 60% of the base substitutions occurred at G:C base pairs in the *gpt* genes. The G:C to C:G transversion was commonly increased by these particle instillations.

Conclusion: Manufactured nano/microparticles, CB, C_{60} and kaolin, were shown to be genotoxic in *in vitro* and *in vivo* assay systems.

Background

Nano/microparticles are widely used because of their desirable properties in industrial, medical and cosmetic fields [1-6]. Accordingly, these particles can be released into the human environment and then can be inhaled. Most exposure to airborne nano/micromaterials occurs in the work place. Nano/microparticles can be classified into three groups: natural, anthropogenic and man-made (or artificial). The natural kind, for example, is produced during forest fires or volcanic eruptions. Anthropogenic particles are quite often a by-product of industrial activities such as welding or polishing. Diesel exhaust products, PM10 and PM2.5, well known as combustion nanoparticles, also belong to this group. The man-made group includes engineered nanomaterials [5].

Among these nano/mocroparticles, diesel exhaust particles have been well documented, in their general toxicity, mutagenicity and carcinogenicity [7-10]. In addition, asbestos, a naturally occurring nano-sized silicate mineral fiber, has been considered to be a human carcinogen [11-13]. Animal experiments and epidemiological studies have already demonstrated that pulmonary fibrosis, bronchogenic carcinomas and malignant mesotheliomas are closely associated with asbestos exposure. Another mineral fiber, titanium dioxide (TiO_2) has also been subjected to extensive research, and TiO_2 has already been shown to be carcinogenic [14]. Moreover, man-made vitreous fibres, including glass fibres, refractory ceramic fibres, and rock wool, have been sorted as carcinogens [15]. Kaolin/kaolinite is a clay mineral with the chemical composition $Al_2Si_2O_5(OH)_4$, and is used in ceramics, medicines, food additives, toothpaste and cosmetics. The largest use of kaolin is in the production of paper [3]. In 1993, W. B. Bunn 3rd *et al.* reported that increased incidences of lung tumors and mesotheliomas were observed in long-term inhalation studies of rats and hamsters treated with micro-sized refractory ceramic fibres containing kaolin as the main component [16]. However, other genotoxic and carcinogenic potentials of kaolin have not been studied *in vitro* and *in vivo*. In addition, the mechanism of cancer development by kaolin is still unclear.

On the other hand, carbon black (CB), fullerenes (C_{60}) and carbon nanotubes (CNTs) are developed as engineered nanoproducts [1,2,6,17]. Despite their highly desirable structures, their toxicity and carcinogenicity are concerns because these engineered nanoproducts are considered to be very stable and could lead to continuous inflammation when deposited in tissues. CNTs especially have received much attention from the aspect of toxicity due to their asbestos-like rod-shaped particles, and iron content [17-19]. Recently Takagi *et al.* demonstrated that multi-wall carbon nanotubes induced mesothelioma in *p53*+/- mice by a single i.p. injection [20]. In contrast, C_{60} is a spherical molecule consisting entirely of carbon atoms, and various derivatives have been reported [6,21,22]. C_{60} has widely different properties, such as scavenging of reactive oxygen species, direct interaction with biomolecules and radical formation; however, clear genotoxic and carcinogenic effects have not yet been demonstrated.

The present study aims to examine the genotoxicity/clastogenicity of widely distributed nano/microparticles such as C_{60}, CB and kaolin by an *in vitro* micronucleus test. Moreover, we analyzed the genotoxic effects of these particles by an *in vivo* comet assay and mutation assay system using *gpt* delta transgenic mice. In this mouse model, point mutations and deletions are separately analyzable by *gpt* and Spi- selections, respectively [23,24]. The mutation assay using the *gpt* delta mouse was validated and so far is widely used in the field of environmental mutagenicity.

Results

Size distribution and agglomeration state in suspensions of nano/microparticles

Figure 1 shows representative transmission electron microscope (TEM) images for the state of test materials

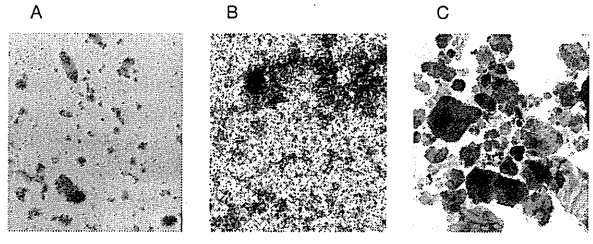

Figure 1
Representative TEM images of the presently used nano/microparticles within the suspensions. C_{60} (Panel A), CB (Panel B) and kaolin (Panel C) were suspended in saline containing 0.05% Tween 80 at a concentration of 2 mg/mL with a 10 min sonication. All images are shown at the original magnification of × 10,000.